T.C.

MARMARA UNIVERSITY

INSTITUTE FOR GRADUATE STUDIES IN

PURE AND APPLIED SCIENCES

MODELING OF METAL COMPLEXES DESIGNED FOR HOMOGENEOUS CATALYSIS

Figen KAYAR AYNALI

(524510004)

THESIS

FOR THE DEGREE OF MASTER OF SCIENCE

IN

CHEMICAL ENGINEERING

SUPERVISOR

Asst.Prof. Dr. Gökçen Alev ALTUN ÇİFTÇİOĞLU

İSTANBUL 2012

MARMARA UNIVERSITY

THE INSTITUTE FOR

GRADUATE STUDIES IN PURE AND APPLIED SCIENCES

ACCEPTANCE AND APPROVAL DOCUMENT

The jury established by the Executive Board of the INSTITUTE FOR GRADUATE STUDIES IN PURE AND APPLIED SCIENCES on ..... (Resolution no:.....) has accepted Ms Figen KAYAR AYNALI's thesis titled "**Modeling Of Metal Complexes Designed For Homogeneous Catalysis**" as Master of Science thesis in chemical engineering.

Advisor : Asst.Prof.Dr. Gökçen ALTUN ÇİFTÇİOĞLU

1. Member of the jury: (Prof. Dr. M.A.Neşet KADIRGAN) (Marmara Üni.)

2. Member of the jury: (Prof.Dr.Mustafa BULUT) (Marmara Üni.)

Date : 19/06/2012

APPROVAL

Ms. Figen KAYAR AYNALI has satisfactorily completed the requirements for the degree of Master of Science in Chemical Engineering at Marmara University. The Executive Commitee approves that he/she be granted the degree of Master of Science on… ……(Resolution no:…..)

DIRECTOR OF THE INSTITUTE

Prof. Dr. Meral Ünal

ACKNOWLEDGEMENTS

This thesis would not been possible without the help of my advisor, my colleagues, my supporting friends, and my family. I would like to take this opportunity to express my deep appreciation to all those who helped me in this hard, but extremely rewarding process.

I would like to express my appreciation to my thesis supervisor Asst.Prof. Dr. Gökçen ALTUN ÇİFTÇİOĞLU for her encouragement, guidance and discussions in my study.

I am also very thankful to Prof. Dr. Zikri ALTUN and Prof. Dr. Carl TRINDLE for valuable suggestions and their guidance when I was not confident enough to proceed. I am very grateful to İlhan YAVUZ for his help in the calculation processes.

I am very grateful to Prof. Dr. M. A. Neşet KADIRGAN for showing support and sharing his experience in composite materials.

I would also take this opportunity to express my appreciation to Prof. Dr. Nahit AKTAŞ for showing his support to me all the time.

At last, I like to thank my family for always being with me. Especially, I am very grateful to my mother Hüsniye KAYAR, who always stood beside me in difficult times. I am very blessed to my father Gülabi KAYAR who always believed in me. I would also like to thank my sister and brother Okan KAYAR and Funda KAYAR for always looking out for me and making me feel safe.

I am deeply grateful to my friend and my dearest husband Cem AYNALI who really helped during my research and showed patience during my work. He was always there for me and helped a lot in editing the data I have evaluated in my studies.

June, 2012 **Figen KAYAR AYNALI**

CONTENTS

ÖZET

HOMOJEN KATALİZ İÇİN METAL KOMPLEKSLERİN MODELLENMESİ

Kataliz reaksiyonları sanayi boyutlarında kimyasal değişimlerin gözlemlendiği proseslerin en minimum enerji kullanılarak yapılabilmesinde en önemli rolü üstlenmektedir. Enerjininin minimuma indirgenmesinde kullanılan en yaygın katalizörler ise metal oksitler olarak rastlanmaktadır. Doğal gazın (metan) kısmi oksidasyonu sonucu elde edilebilecek kolay taşınabilir metanolün C-H bağ aktivasyonu homojen katalizör kullanılarak araştırılmıştır. Dehidrojenasyon ve dehidrasyon reaksiyonları OsO^+ metal oksit katalizörü kullanılarak metanın aktivasyonu Gaussian 09 ve ADF programları kullanılarak teorik olarak incelenmiştir. İncelenen reaksiyonun gibbs oluşum enerjisinin değişimi elde edilmiştir. Ek olarak Arrhenius grafikleri tüm sunulan reaksiyonlar için elde edilmiş ve aktivasyon enerji değerleri hesaplanmıştır.

Haziran, 2012 **Figen KAYAR AYNALI**

ABSTRACT

MODELING OF METAL COMPLEXES DESIGNED FOR HOMOGENEOUS CATALYSIS

Catalysis is the key toward accomplishment of industrially significant chemical transformations with minimum energy investment. Transition-metal oxides are one of the common catalysis in oxidation process used to minimize energy investment. The C-H bond activation to form the easily transported liquid fuel methanol from partial oxidation of natural gas (methane) using homogenous catalysis was investigated. The reaction mechanism of the dehydrogenation and dehydration has been investigated theoretically for the activation of methane by OsO^+ using Gaussian 09 software and ADF software. The change of the formation gibbs energy of the reactions under investigation has been obtained. In addition, Arrhenius plots of all the proposed reaction were presented along with the calculated corresponding activation energies.

June, 2012 **Figen KAYAR AYNALI**

SYMBOLS

°C, K : Temperature

s^{-1} : Velocity

kcal/mol : Energy

cm^{-1} : Frequency

ABBREVIATION

DFT : Density Functional Theory

TS : Transition State

ADF : Amsterdam Density Functionals

LNG : Liquified Petroleum Gas

CNG : Compressed Natural Gas (CNG)

PES : Potential Energy Surface

k : The reaction rate coefficient

Ea : Activation Energy

R : The universal gas constant

T : Temperature

V : Volume

M : Metal

S : Substrate

L : Ligand

ZPE : Zero Point Energy

Ee : Electronic energy

Er : Rotational energy

Ev : Vibrational energy

Etr : Torsional energy

IR : Infrared

B3LYP : Becke, three-parameter, Lee-Yang-Parr exchange-correlation functional

B3PW91 : The non-local correlation provided by Perdew/Wang 91.

GGA : Generalized gradient approximations

LDA : Local-density approximation

ΔS : The change of entropy

ΔH : The change of enthaply

ΔG : The change of gibbs free energy

ΔH_f^O : Formation of enthalpy

ΔG_f^O : Formation of gibbs free energy

LIST OF FIGURES

PAGE NO

LIST OF TABLES

PAGE NO

CHAPTER 1: INTRODUCTION

The importance of natural gas as a raw material for the chemical industry is becoming more apparent as the predicted abundance of oil reserves declines over the long run. Methane is probably the most abundant natural gas on earth, but is often deposited in inaccessible areas both onshore and offshore. Even when a potential natural gas reservoir is found, very heavy costs of exploration and drilling must be borne to make it available for use by the general public. There is often considerable waste in handling the gas. We all have seen flames over oil wells, from natural gas combustion. Burning not only consumes a valuable hydrocarbon, it produces a significant amount of carbon dioxide (CO_2), a greenhouse gas. The natural gas must be converted to more compact form, either liquefied natural gas (LNG) or compressed natural gas (CNG) before it is transported to areas where needed. This is also a very costly and time consuming process. The costs of transportation and storage would be much reduced if natural gas could be converted at the collection site into more easily handled materials that are liquids at normal conditions, such as methanol or other hydrocarbons. These can easily be transported from remote area to consumers for either direct use or as a chemical feedstock for subsequent transformations. If public resistance to nuclear energy remains strong, natural gas is likely to become a more important energy source.

Industrially, methanol production from methane is being realized a high temperature process called “cracking” which accomplishes partial oxidation of the CH_4 to hydrogen gas and carbon monoxide. Unfortunately the cracking and conversion efficiency is as low as five to ten percent [1]. Discovery of more effective catalysts is becoming more urgent as the demand for clean energy grows across the world and concern becomes more widespread about climate change related to enhancement of global warming due to emissions of greenhouse gases.

Both heterogeneous (multiphase) and homogeneous (monophase) catalysis are found to be very promising for catalytic conversion of methane to methanol. Many of the transition metals behave as catalysts, either as the metal itself or as a compound. Over the last 15 to 20 years academic and industrial research together in this area has greatly expanded the scope of catalytic reactions of high efficiency. A large number of different types of ligands and their transition metal complexes have been developed in hopes of improving the homogeneous catalysis of various organic transformations. It looks that the research efforts in this area will grow with

accelerated speed for many years to come since the results are of direct concern for life on earth.

Here we give special attention to catalysts capable of activating C-H bonds so to ease partial oxidation of hydrocarbons. Although the transition-metal oxides serving as catalysts in such oxidation processes are generally in the solid phase and the reactant(s) undergoing transformations on their surface are generally drawn from gas or liquid phase it is still possible to model such details as the C-H bond activation by assuming all the constituents are in the gas phase. It appears that activation does not depend on solvent, surface inhomogeneity, and aggregation effects occurring on surfaces or in solutions. From the stand point of the C-H bond activation the reaction can be treated as a homogenous catalytic reaction and transition metal oxide can be looked at as a homogeneous catalyst. In this thesis medium effects on OsO catalysis are not considered in computational modeling. The effects of composition, stoichiometry, size, charge state, and degree of coordinative saturation, which are among the most important factors affecting catalytic properties, can all be studied using computational quantum chemistry. There has been a growing number of experimental and theoretical studies on the activation of small hydrocarbons such as methane by various transition-metal ions, transition-metal oxide ions, and transition-metal oxide cluster ions in the gas phase. The density functional method (DFT) have been used in modeling heterogeneous and homogenous catalysisl it has successfully simulated the structures, bonding, and spectra in transition metal complexes of medium size [1-5]. Theoretical modeling of the catalytic effect of transition metal complexes is already vigorously pursued by DFT computations conducted by a number of established investigators [6-10]. DFT incorporates terms in its energy expressions (called functionals) that depend on the gradient of the density to improve the contribution of exchange interactions in the correlation energy [2]. These "gradient-corrected" functionals are especially well suited to the task of describing the catalytic action of metal complexes, and are used in most modern studies.

Despite the concentrated effort to provide computational descriptions of transition metal complex participation in reaction pathways, there is considerably more experimental data in need of analysis than has been successfully explained at the molecular/electronic level. There is opportunity for an important work in the investigation of C-H bond activation, which can be readily obtained in the gas phase, to replace one H or two H atoms with a hydroxyl group.

This study contributes to the understanding of the C-H bond activation to form the easily transported liquid fuel methanol from partial oxidation of natural gas (methane) using homogenous catalysis. This has received considerable attention both experimentally and theoretically. Many theoretical investigations on the mechanisms of the of the reactions of bare metal and monomeric metal oxide ions (MO^+) with CH_4 have been reported. The detailed PESs have been obtained for ScO^+, TiO^+, VO^+, CrO^+, MnO^+, FeO^+ and FeO^{2+}, CoO^+, NiO^+, CuO^+, PtO^+ with CH_4 to produce methanol or methyl [9, 11 a, b].

In this study, the reaction mechanism of the dehydrogenation and dehydration has been investigated theoretically the activation of methane by second- and third-row transition-metal oxide ions and metal oxide cluster ions. Specifically, dehydrogenation or dehydration of methane by osmium oxide cations has been theoretically explored using Gaussian 09 software and ADF software.

On the other hand, this will be the first report of the change of the formation gibbs energy of the reactions investigated in this study. In addition, Arrhenius plots of all the proposed reactions were presented along with the calculated corresponding activation energies.

CHAPTER II. CATALYSIS

Catalysis is the change in the rate of a chemical reaction due to the participation of a catalyst that is an additive used in substoichiometric amount to manage a reaction at a temperature below that required for the uncatalyzed thermal reaction.

Unlike other reagents that participate in the chemical reaction, a catalyst itself remains unchanged during the catalytic conversion. It binds the reactants,or substrates,for the catalytic reaction and then liberates the products to regenerate the catalyst and typically, a catalyst may participate in the catalytic cycle 101-106 times or more,allowing its use in modest or even trace amount [1].

The catalyst increases the reaction rate which is related to chemical kinetics [2- 8]. A study into the kinetics of a chemical reaction is usually carried out with one or both of two main goals in mind [7]:

1. Analysis of the sequence of elementary steps giving rise to the overall reaction. i.e. the reaction mechanism.

2. Determination of the absolute rate of the reaction and/or its individual elementary steps.

The term rate of reaction means the rate at which reactants are used up, or equivalently the rate at which products are formed. To measure a reaction rate, ne needed to monitor the concentration of one of the reactants or products as a function of time. The rate is proportional to the concentrations of the reactants as Eq. II.1:

$$\nu = k\, a[\mathrm{A}]b[\mathrm{B}]c[\mathrm{C}] \qquad \textbf{(II.1)}$$

where the specific rate *k, rate constant,* is independent of concentration but does depend on temperature, catalysts, and other factors. The effect of temperature on rate constant, k, is given by Arrhenius, Eq. II.2:

$$k = A \exp(-E_a/RT) \text{ or equivalently } \ln k = \ln A - Ea/RT \qquad \textbf{(II.2)}$$

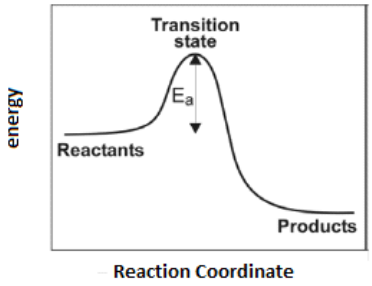

Figure II.1 Energy coordinate versus energy

where E_a is the activation energy for the reaction, and A is a constant known as the preexponential factor. These parameters may be determined from experimental rate data by plotting ln$k$ against 1/T. This is known as an Arrhenius plot, and has an intercept of ln$A$ and a slope of $-E_a/R$.

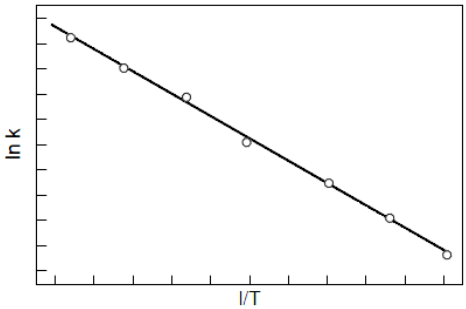

Figure II.2 The Arrhenius Plot.

This temperature dependence means that in order to measure an accurate value for k, the temperature of the reaction mixture must be maintained at a constant, known value. If activation energies are to be measured as part of the kinetic study, rate constants must be measured at a series of temperatures. Another Arrhenius-like expression appears in the "transition state theory" of chemical reactions, formulated by Wigner, Eyring, Polanyi and Evans in the 1930s. This takes various forms, but one of the most common is [2]:

$$k = \frac{kT}{h} exp\left(\Delta S^{\#}/R - \Delta H^{\#}/_{RT}\right) = k_o exp\left(E_a/_{RT}\right) \qquad \textbf{(II.3)}$$

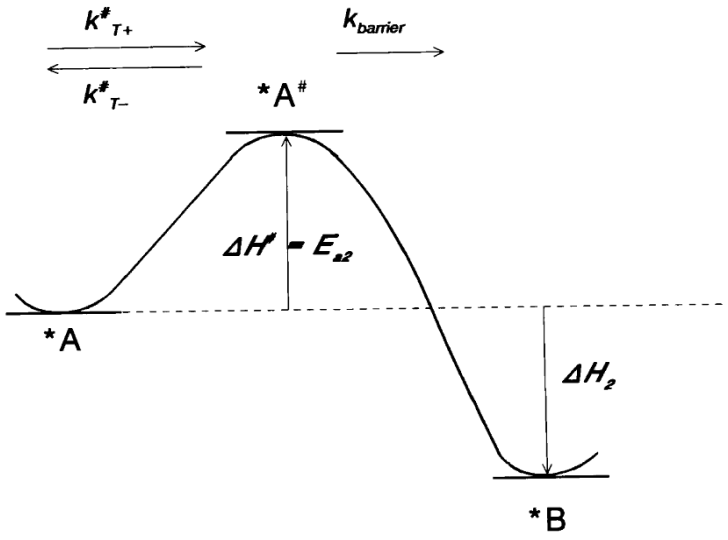

Figure II.3 Energy diagram for the rate determining surface reaction [2].

According to the transition state theory, the reaction rate of the rate determining step can be computed from Eq. III.4.

$$k_T = k_{barrier} K_T^{\#} = k_{barrier} \left(\frac{k_{T+}^{\#}}{k_{T-}^{\#}}\right) \quad \textbf{(II.4)}$$

It is assumed that the reacting complex is in equilibrium with the transition state (TS) complex and that the number of molecules in the transition state that react to give the product per unit of time is given by the frequency $k_{barrier}$. The rate of this step is assumed to be rate limiting. It implies that energy exchange is fast compared to the overall reaction rate. This is depicted in Fig. II.1**.** Because $K^{\#}_T$ is an equilibrium constant it can be written as in Eq. III.5**,** where $\Delta G^{\#}$, $\Delta H^{\#}$ and $\Delta S^{\#}$ are the free enthalpy, the enthalpy and the entropy differences between the transition state and the ground state, respectively [2].

$$K_T^{\#} = exp\left(\frac{-\Delta G^{\#}}{RT}\right) = exp\left(\frac{\Delta S^{\#}}{R} - \frac{\Delta H^{\#}}{RT}\right) \quad \textbf{(II.5)}$$

As long as quantum-mechanical corrections can be ignored:

$$k_{barrier} = \frac{kT}{h} \quad \textbf{(II.6)}$$

For the rate constant of the rate determining step this results in Eq. II.3. $\Delta H^{\#}$ can be identified approximately with the activation energy E_a of the reaction step,

and $\Delta S^{\#}$ with the entropy of activation. However while a catalyst increases the rate of a reaction, it does not change the extent of a reaction. This means that it does not effect the chemical equilibrium of a reaction, because the rate of both the forward and reverse reactions are affected. It lowers the barrier of activation of a reaction by providing an alternative pathway, which may involve many intermediates and many steps to the reaction product. The rate of the reaction is increased at the same temperature as this alternative route has lower activation energy than the corresponding uncatalyzed reaction. However the mechanistic explanation of catalysis is complex. The sequence of steps are called as the mechanism of the reaction and this mechanism refers to the more detailed description of a reaction at the molecular bonding level.

In Fig. II.4a, the substrate S is slightly less stable than the product P so the reaction will stable than the product P, so the reaction will eventually reach an equilibrium favoring P. Also Fig. II.4 ensures that the product is thermochemically more stable than the starting materials and so the reaction is indeed favorable [1]. The substrate binds to the metal and the substrate -catalyst complex is represented as "M.S" in Fig. II.4. The binding between catalyst and substrate is not strong. If the bonding is too strong the complex 'M.S' will be too stale and the activation energy to get to "M-TS" will be just as large as the activation energy in the uncatalyzed reaction which has the pathway from S to TS. Also S can not bind too weakly because it may be excluded from the metal and not managed to be activated by the metal. Similarly, the product P will normally be formed as the complex "M.P". Product P musn't bind to catalyst weakly because of possibility of displacing S with P, so the catalyst will be effectively poisoned by the products of the reaction. For most transition metal catalysts, the catalyzed reaction goes by a multistep mechanism instead of passing by way of the high energy uncatalyzed transition state TS as shown in Fig. II.4a. In the catalysed reactions,metal stabilizes intermediates and they are stable only when bind to the metal. This means that, M-TS complex occurs. Thus, we can say that M-TS is much more favorable than TS and the reaction passes through the catalyzed route. Fig. II.4b shows a schematic catalytic cycle. The active catalyst M is often rather unstable and is only formed in situ from the catalyst precursor [1].

The use of a catalyst also often imparts a degree of selectivity to one or more reaction products, when compared to the uncatalysed reaction. This is an important

concept in catalysis, and along with the ability to increase the rate of reaction, both can be manipulated by selection and modification of the catalyst.

In conclusion, the use of a catalyst provides a lot of advantages which will be explained in details in the preceeding sections.

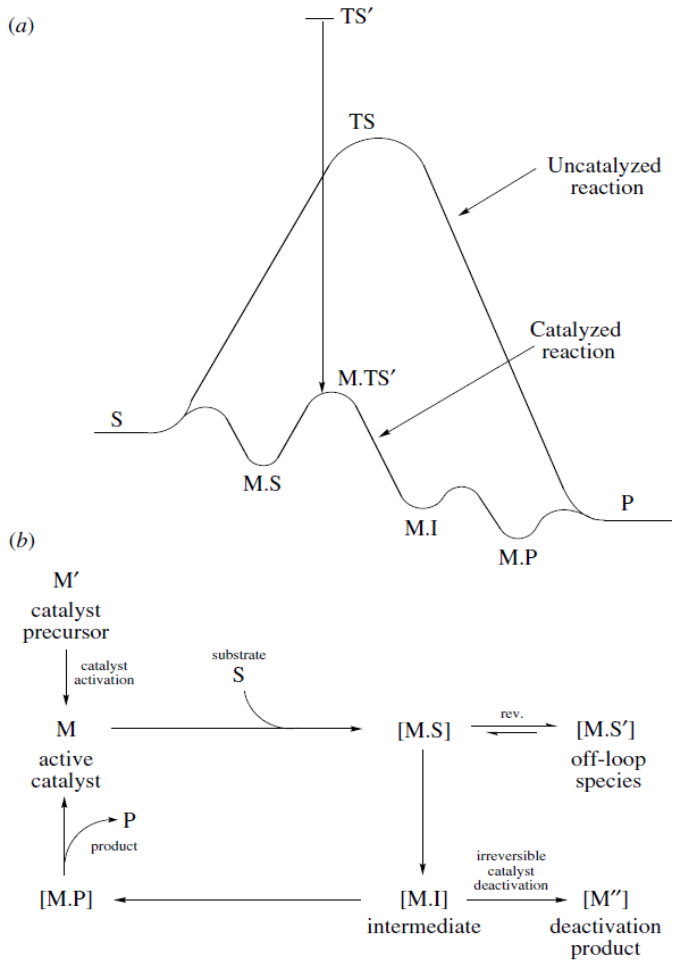

Figure II.4 For most transition metal catalysts, the catalyzed pathway is completely changed from the pathway of the uncatalyzed reaction [1].

(*a*) A catalyst lowers the activation energy for a chemical reaction. Here the uncatalyzed conversion of substrate S to product P passes by way of the high-energy transition state TS. In this case the metal-catalyzed version goes via a different transition state TS' which is very unstable in the free state but becomes viable on binding to the catalyst as M.TS'. The arrow represents the M−TS' binding energy. The uncatalyzed and catalyzed processes do not necessarily lead to the same product as is the case here. b) Typical catalytic cycle in schematic form [1].

II.1 THE HISTORY OF CATALYSIS

Catalysis was practised by many early societies without realizing its impact as demonstrated by the production of wine and beer (fermentation),soap,cheese,sulfuric acid and ether. In the middle ages sulfuric acid was synthesized in small quantities in glass equipment by burning sulphur with nitric acid in humid air. In 1746, lead was used as a construction material for the reaction chambers and larger production volumes became possible. In 1793, Clement and Desormes showed that the quantity of nitre could be reduced by admitting additional air to the reactor. They were aware of the fact that the nitrous vapors are only intermediates and the oxidazing agent is air [2].

Catalysis emerged from scientists seeking to understand the chemistry and the origin of the promotion by catalytic materials. In the second half of the eighteenth century there were various reports of what we would recognize today as catalytic reactions. However, the idea of a catalytic reaction could not have been understood before chemical elements and chemical change had appeared. The idea of catalysis can be taken as starting in 1814 when Kirchoff published his work on the hydrolysis of starch to glucose by acids. A number of people had investigated the hydrolysis, but Kirchoff was the first clearly to understand what was going on [12]. The phrase "catalyzed processes" was coined by Swedish chemist J. J. Berzelius in 1836 when he noticed changes in reactions that were accelerated by substances that remain unchanged after the reaction. In a short paper summarising his ideas on catalysis as a new force,he wrote: “It is, then, proved that several simple or compound bodies, soluble and insoluble, have the property of exercising on other bodies an action very different from chemical affinity. By means of this action they produce, in these bodies, decompositions of their elements and different recombinations of these same elements to which they remain indifferent.” Berzelius proceeded to propose the existence of a new force which he called the “catalytic force” and he called “catalysis” the decomposition of bodies by this force. This is probably the first recognition of catalysis as a wide-ranging natural phenomenon [13].

An important event in the development of catalysis came in 1817 when Humphry Davy discovered the oxidation of hydrocarbon gases on platinum. The oxidation of coal gas was catalyzed by platinum wire. That chemical reaction which carries out between two gaseous reactants can occur on a metal surface with the

metal being chemically unchanged. Only platinum and palladium wires were effective; wires of copper, silver, gold and iron were ineffective. This the heterogeneous catalytic processes that were first recognized [12,13]. Edmund Davy,who is Humphry Davy's cousin continued the work and in 1820 he discovered that the platinum could be introduced at room temperature provided that it was finely divided. Döbereiner continued this work and in 1823, he found that, in the presence of platinum, vapors of ethanol reacted with oxygen to form acetic acid. Work on selective oxidation continues to this day but Döbereiner did it first. He also noticed, in line with the work of Edmund Davy, that divided platinum became red hot in the presence of hydrogen and oxygen [12].

Another line of catalytic work was started by Thenard. In 1813, Louis Jacques Thenard discovered that ammonia is decomposed into nitrogen and hydrogen in contact with metals, provided they are hot. Ten years later, with Pierre Dulong, he found that the activity of iron, copper, silver, gold, and platinum for decomposing ammonia decreased in the order given. This is one of the earliest recorded examples of a pattern of catalytic activity [12,14]. Later, he systematically studied the dissociation of hydrogen peroxide. He concluded that a chemical reaction can be speed up with a chemical substance which are not chemically changed. In 1834,Faraday proposed simultaneous adsorption of reactants on a platinum surface but he did not really explain the catalytic action. Organic heterogeneous catalysis remained unexplored for many years after 1834. However, the beginning of the technology of heterogeneous catalysis came in this period [12]. The Deacon process was developed in the 1860's - the oxidation of hydrogen chloride to chlorine on copper chloride.

$$2HCl + ½\ O_2 \longrightarrow H_2O + Cl_2 \qquad \textbf{(II.7)}$$

Messel started the first plant for the oxidation of sulfur dioxide tosulfur trioxide in 1875.

$$SO_2 \longrightarrow SO_3 \qquad \textbf{(II.8)}$$

In 1888, Ludwig Mond discovered steam reforming of hydrocarbons on nickel/pumice to give carbon monoxide and hydrogen.

$$CH_4 + H_2O \longrightarrow CO + 3H_2\ (Ni) \qquad \textbf{(II.9)}$$

At the end of the eighteenth and the beginning of the nineteenth century,the influence of metals and oxides on the decomposition of several substances was studied by many scientists. For example, Joseph Priestley, the discoverer of oxygen, and the Dutch chemist Martinus van Marum made observations on the dehydrogenation of alcohol on metal catalysts. It was noticed that with different substances gives very different products. An example is the decomposition of alcohol: in the presence of copper or iron, carbon and an inflammable gas is produced. In the presence of pumice stone decomposition into ethene and water was observed. In other words, selectivity was demonstrated [2].

In 1895,Wilhelm Ostwald at Leipzig University started a systematic investigation into reactions that were catalyzed by the presence of acids and bases and found that chemical reactions occur at finite rates and these rates can be used to determine the strengths of acids and bases. For this work Ostwald was awarded the 1909 Nobel Prize in Chemistry [2]. Ostwald gave the definition that we use until today: "A catalyst is a substance that changes rate of a chemical reaction without itself appearing into the products" [4].

Here,a few catalysts first emerged for the production of large volumes of key chemicals listed [14] :

- SO_2 oxidation by the Contact Process in 1831.
- Sulfuric acid production enhanced by use of V_2O_5 in 1875
- Nitric acid production enhanced by the use of Pt gauzes in 1904
- NH_3 synthesis from N_2 and H_2 in 1905; at a large scale at BASF in 1910
- Methanol synthesis developed by BASF in 1923 at high pressure over a ZnO-chromia catalyst.
- Fischer-Tropsch synthesis of synthetic fuels commercialized in 1930 as an alternative to processing heavy oil.

In fact, at the early history of catalysis was focused at to creative individuals largely in academia seeking to understand how catalysts influenced chemistry. After because of the demand for the production of these catalyzed chemicals in sufficient quality and quantities, also at a reasonable cost was emerged. Some industrial companies (Dow, GE, DuPont, BASF, ICI, Monsanto, etc.) generated their own fundamental research labs in the 1940s through the 1970s often with contact with academic based centers to not only discover catalysts, but also to develop and commercialize them. For over the last 250 years, from 18^{th} into the 21^{st} century,

industry have played crucial role at producing catalysts. Especially with the advent of petroleum as a fuel in the 20th century, tremendous growth of catalysis research was seen with the rapid increasing in 1940s. Huge industries emerged around producing products to enhance our quality of life through plastics, pharmaceuticals and specialty chemicals via development of a petrochemicals industry.

Some examples on these catalysis are that [14] :

- Oxidation of benzene and aromatics to anhydrides in 1920 over V_2O_5.
- Isopropanol, the first bulk chemical produced from petroleum, from refinery propylene over an acid catalyst , in 1920 by standard oil of New Jersey.
- Producing of H_2 by steam reforming in 1930 for use in refineries.
- Ethylene oxide with Ag/alumina in 1937.
- In 1938, Otto Roelen discovered oxo synthesis while working at Fischer's Kaiser Wilhelm Institute for coal research.
- Eugene Houdry who was a mechanical engineer in France pioneered the use of clay catalysts and the engineering of continuous unit operations.
- In the 1960s the approach of cracking of molecules in the presence of H_2 (hydrocracking) originally used in Germany from 1915 to 1945 to crack coal based feeds was revived beginning with Chevron using metal promoted silica-aluminas, aluminas and later zeolits.

However with the development of a petrochemicals industry, the transportation industry emerged in 20th century to refine petroleum products into fuel feedstocks via [14] :

- Alkylation of olefins and isomerization paraffins with $AlCl_3$ in 1932.
- Catalytic cracking in 1936.
- Naphtha reforming in 1950.
- Friedel-Crafts for cumune production and later zeolits.
- Oxychlorination in 1964.
- Zeolitic cracking and hydrocracking in 1964.
- Multi-metallic reforming in 1967.
- Dewaxing and hydroprocessing.

The growth of the transportation industry, industrial activity and a severe increase in environmental pollutants resulted in the creation a new industry using

catalysts to control vehicle and stationary engine emissions. Today sales of environmental catalysts comprise almost one third of the $16 billion catalyst business. These commercialized events include [14]:

- Hydrodesulfurization in 1960s, a extremely important method for removal of sulphur from fuels resulted in considerable reduction in global emissions of sulfur oxides.
- Selective catalytic reduction of NO_X by NH_3 for powerplants in 1980 using V,W and Ti oxides.
- Reduction of ozone generating chlorofluorocarbons.
- Diesel oxidation exhaust catalysts in 1990 using cerium only.
- Variety of solutions using metal oxides for catalytic decomposition of N_2O which resulted in an 81 % reduction of all N_2O emissions from the world's adipic acid plants.
- Pt-Rh-alkali NO_X storage catalysts, Toyota Motor, 1994.
- Diesel particulate catalysts in 2003.
- Urea SCR (semiconductor-controlled rectifier) for NO_X emissions control in mobile vehicles, 2004.
- NO_X removal in FCC (Fluid Catalytic Cracking) regenerator units, 2007.

In adddition to need for like transportation and emissions control, the discovery and development of zeolit molecular sieves stimulated the discovery of many novel and selective catalytic processes. Zeolits were used in large volumes to enhance the catalytic cracking and hydrocracking of petroleum feedstocks and the

- Production of chemicals and fuels.
- Dewaxing of distillates and lubebase feeds
- Oligomerization of olefins.
- Xylene synthesis and isomerization.
- Ethyl benzene and PET, and
- Gasoline and light olefins from methanol, 1976.

Thus we see the history of industrial catalysis in the last 250 years is still growing. Today over 90% of all industrial chemicals are produced with the aid of catalysts. We have seen catalysts evolve into new industries, such as

- Electrocatalysis,
- Fuel cells,

- Photocatalysis,
- Phase transfer catalysis.

II.2 THE ADVANTAGE OF CATALYSIS

As we know the catalyst increases the rate of a process. Rates represent a cost factor: higher rates allowing higher space-time yields (kg of product per time and reactor volume)and hence smaller reaction vessels. Also higher rates and higher overall catalyst yields (mass of product per unit mass of catalyst) reduce the catalyst costs per unit mass of product generated.

One of the most important criteria for judging a catalyst is its selectivity. Higher selectivity for the desired product minimizes product separation problems and do not need to discard the undesired product as waste. Higher selectivity is a means [4] :

- to reduce waste,
- to reduce the work-up equipment of a plant, and
- to ensure a more effective use of the feedstocks.

Shortly we can say that, a high selectivity is essential for an ecological as well as economical process.

As be told in history of catalysis, the catalysts play a key role in the petrochemicals industry and this industry manufactures all kind of important chemicals from production of energy in fixed (power stations) or mobile (vehicles) installations to building blocks for a wide rate variety of plastics through lubricating and other oils, the main components shampoos, detergents, soap, perfumes etc. [15]. Briefly they have a great extent in our life, but there is a big problem. The industries that rely on petrochemicals produces large amounts of waste more than the amount desirable material and elimination of waste is the biggest challenge to face. Catalysts were used to handle this challenge because of having high selectivity. Also alternative fuels seen as an important alternative to conventional fuels include: fossil fuels (petroleum (oil), coal, propane, and natural gas as well as nuclear materials such as uranium and thorium which cause environmental pollution largely dependent on catalysts.

Another advantage of a catalyst is that it allows reactions to be carried out under milder conditions. This means by bringing a reaction at lower temperature a catalyst can save energy in commercial applications.

The increasing efficiencies, quality and quantity of processes driven by feedstock, energy and environment can be ascribed to improvements in catalytic systems. Especially in the future, catalysts will have a big impact to environmental catalysis by increasing sulfur and NO_X emissions, decreasing CO_2 levels. Moreover, may be the most of our automotive exhaust gases will be cleaned by a catalyst. However catalysts will contribute to water purification and recycle, the decomposition of water and perhaps even solar conversion of CO_2 into CHO_X. These all cause increasing interest in the catalysis processes to improve our understanding, testing and development of these processes by using theory and modeling of new catalysts [2,14].

II.3 HOMOGENEOUS VERSUS HETEROGENEOUS CATALYSIS

Although enzymes were used in some processes in early history for fairly large volume products such as the synthesis of polylactide they are not used at present, because of their low selectivity to a desired product as well as their often low stability under conditions except for those which they were optimized (room temperature, atmospheric pressure). Therefore, manmade catalysts have been introduced. Especially there has been an upsurge of research in the area of catalysis by metal complexes since 1940s [15,16]. Several factors contribute the great catalytic versatility of transition metal complexes in the reactions [17] :

- The existence of relatively stable but highly reactive complexes of transition metals which, by virtue of their electron configurations and coordination numbers, exhibit reactivities closely related to those the 'reactive intermediates' of organic chemistry namely, free radicals, carbenes, and carbanions.
- The ability of transition metals to stabilize a variety of unstable reaction intermediates through coordination as ligands in relatively stable but reactive complexes.
- The ability of certain transition metal complexes to promote rearrangements within their coordination shells by virtue of the existence of two or more stable configurations of the complex differing

in coordination number and/or oxidation number.

- The ability of a transition metal atom to assemble and/or to orient several component of reaction within the framework of its coordination shell (template effect). An example of reactions in which this effect is probably important is :

The catalysis of the cyclotrimerization of butadiene to 1,5,9-cyclododecatriene (CDT) by cyclododecatrienenickel, reported by Wilke,

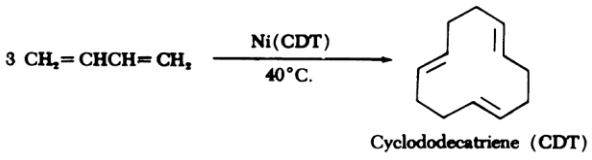

(II.10)

The catalysis by metal complexes is an exciting, fast developing and challenging interdisciplinary topic which includes homogeneous and heterogeneous catalysis. Traditionally homogeneous and heterogeneous catalysis are separate disciplines. The term homogeneous catalysts are used due to catalysts and substrates for the reaction are used in the same phase. In contrast, heterogeneous catalysis takes place at the surface of a solid catalyst. To a large extent catalysis is concerned with the transformations of organic molecules. Homogeneous and heterogeneous (metal) catalysts have been developed in isolation from organic chemistry because the synthesis of a catalytic material requires a knowledge of inorganic and organometallic chemistry, surface science, and spectroscopic techniques. Today, Homogeneous catalysis as a very important research field in Inorganic Chemistry. Majority of homogenous catalytic applications has resulted from development of the organometallic chemistry. This is certainly the area that has led to the largest number of industrial applications in the last three decades. Homogenous transition metal catalysts are used in such industrial processes as [2]:

- toluene oxidation to benzoic acid,
- xylene oxidation to phthalic acid,
- ester condensation to polyesters,
- carbonylation of methanol to acetic acid
- carbonylation of methyl acetate to acetic anhydride
- polymerization of dienes to unsaturated polymers,
- hydroformylation of alkenes to aldehydes

- oligomerisation of ethene and propene,
- hydrocyanation of 1,3-butadiene to adiponitrile,
- asymmetric hydrogenation (e.g. L-DOPA),
- codimerization of 1,3-butadiene and ethene,
- oxidation of ethene to ethanal,
- ring opening metathesis polymerization of dicyclopentadiene and norbornene derivatives,
- hydrosilylation of alkenes

The success of organometallic catalysts are provided by changing the ligand environment easily. By variations in ligands surrounding metal allows optimization of the catalytic activity and large variety of ligands determines the properties of catalysts. However, ligands control the geometric arrangement of the reactive complex intermediates, thus show activity with remarkable selectivity and high selectivity is a significant difference between homogeneous and heterogeneous catalysts [18]. High selectivity increases the purity of the products and reduces the amount of waste, so provides developing a more environmentally friendly industry [10,16]. Thus more researches in recent years focused on homogenous catalysis. Also new knowledge regarding structure and reactivity of organometallic compound has created new catalytic processes in industry or has reestablished old catalytic features under improved conditions. Important examples include the replacement of cobalt by rhodium in a number of industrially otherwise unfeasible processes such as methanol carbonylation and hydroformylation [19].

However homogenous catalysis is one of the most interesting field of chemistry for its mechanism and kinetics. The complications of nonuniform and easily contaminated surfaces make heterogeneous catalysis more difficult to interpret. Homogenous catalysis provides excellent opportunities for the study of the reaction mechanism because it facilitates the job of catalyst optimization and design. (5) So we can say the mechanism of a homogeneous catalytic process can be worked much more easily because it represents better mechanistic understanding of its microscopic processes. The mechanistic ideas developed in homogeneous catalysis make a meaningful contribution to our understanding of field of classical heterogeneous catalysis by suggesting structures for intermediates and mechanism for reaction steps [1,17]. One of the other important differences between homogeneous and heterogeneous catalysis that although in the heterogeneous

catalysis the recovery of catalyst is relatively easy, in homogenous catalysis the catalyst-product separation is a problem. Distillation or crystallization of the product are often very effective, sometimes phase separation or extraction can be used successfully. Another approach is the immobilization of a soluble catalyst on an insoluble carrier that can be separated by filtration [20]. The other difference is the reaction temperature. In contrast to heterogeneous catalysis the reaction can be carried out at low temperature.

Consequently, we can say that for a long time practical catalysis remained an empirical art rather than a scientific discipline, mainly because of the complexity of the catalytic systems. Advanced inorganic and organometallic chemistry have changed catalytic practice and produced significant economic and environmental benefits. Due to that reasons while half of the large scale chemical processes currently in use are based on homogeneous catalyst, the early were mainly based on heterogeneous catalysts [2].

II.3.1 Historical Notes on Homogeneous Catalysis

By far the oldest homogenous catalysts are metallo-enzymes, a metal complex built into a high-molecular weight protein, such as iron porphyrin complexes active for oxidation, zinc complexes for decarboxylation and alcohol dehydrogenase, nickel complexes in hydrogenase enzymesfor hydrogen activation, cobalt corrin (methylcobalamin) complexes for carbon-carbon bond formation, copper imidazole complexes (from histidine) complexes in hemocyanin, etc. [4].

The first industrially applied catalyst working in solution and employing organometallic intermediates is most likely mercury sulfate, which was used for the conversion of acetylene to acetaldehyde in 1920s. In fact homogenous catalysis is the success story of organometallic chemistry. Otto Roelen's initial discovery of hydroformylation in 1938 was followed by systematic research into the catalytic chemistry involving organometallic compounds.

A second process that came on stream in the fifties is the oligomerisation of ethene using cobalt complexes. The origin of modern organo transition metal chemistry can be lied to the discovery of ferrocene in 1951. Since the seventies the proportion of homogeneous catalysts has been increasing with success stories such as that of rhodium catalyzed carbonylation of methanol (Monsanto), rhodium catalyzed hydroformylation (using Wilkinson's findings), Shell's higher olefins process,

asymmetric hydrogenation to L-DOPA (Monsanto), and ring-opening polymerization of cyclooctene using tungsten metathesis catalysts (Huels) [4].

In 1970s, Kaminsky and coworkers discovered the high activity of mixtures of early transition metal complexes containing metallocene ligands and methylalumoxane (MAO) as co catalyst.

Nobel prizes for chemistry have been awarded to Ziegler and Natta (1963), Fischer and Wilkinson (1973) for their discoveries in Organometalic chemistry and homogeneous catalysis. More recently, in 2005, Chauvin, Schrock, and Grubbs and in 2010, Richard F. Heck, Ei-ichi Negishi, Akira Suzuki were awarded for developing organometallic catalysts [15,21].

II.4 METHANE TO METHANOL

Because of recent fluctuations in the price of crude oil in addition to the anthropogenic production of carbon dioxide have resulted in increased interest in energy sources instead of petroleum and coal. Natural gas is an important resource that provides a cleaner resource with the opportunity to reduce CO_2 emissions [22]. Hence, more recently natural gas resources appear to have become more important than had been expected and that gas will play an important role in the future energy supplies of the world. In many respects, methane which is the principle component of most natural gas reserves is an ideal fuel for home and industrial heating as well as for generation of electrical power due to its availability in most populated centers, its ease of purification to remove sulfur compounds and the fact that among the hydrocarbons, it has the largest heat of combustion relative to the amount of CO_2 formed [23,24].

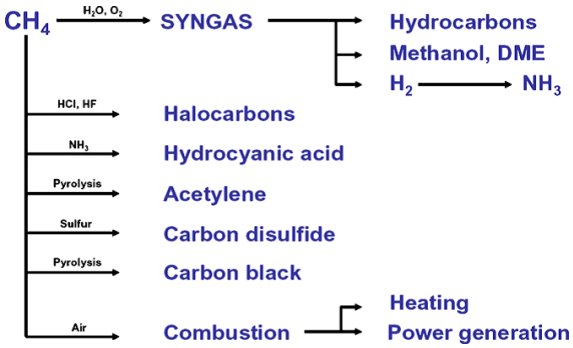

Figure II.5 Methane in industrial processes [11]

But large quantities of the natural gas, substantial methane (the major component of natural gas, ca. 87% by volume) are located in remote areas and its use has been limited by the expense associated with transportation of a flammable, low-boiling gas (-161.8 ^{O}C at pressure of 1 atmosphere). Also compression to form liquid natural gas requires substantial energy input, which limits economic feasibility and has concerns over safety [25,26].

The selective conversion of methane into a transportable liquid (such as methanol) in an economically competitive process is important to transport of methane more safely and cheaply to commercial and population area. However methanol is a clean, renewable fuel and can be used as an intermediate source of energy, particularly in automobiles, fuel cells, space heating, electric power generation and so on. Also because of environmental considerations recently, methanol is being considered as a replacement for methyl tertiary buthyl ether, used as an additive in petrol to increase the oxygen component [27]. But the conversion of methane to methanol or aromatics represents a big challenge because methane is a relatively unreactive. The inert nature of methane is due to its high C-H bond dissociation energy (BDE; ca 104 kcal mol^{-1} ; 1kcal=4,18 kj) and the covalent nature of the C-H bond. As a result, methane is a very weak base, and the coordination of methane to metal catalyst is a substantial challenge [28-30].

Among current processes that convert methane to a liquid is divided in two groups [11,12], as indirectly (via syngas, H_2 + CO) which requires temperature (ca. 900 ^{O}C) and pressure and directly via a catalyst for low temperature ($\leq$ 250 ^{O}C) and pressure.

II.4. 1 The indirect conversion

Rely up on the formation of synthesis gas (H_2 + CO) either by *steam reforming reactions* or *partial oxidation* [22].

Steam reforming is the dominant for production of synthesis gas:

$CH_4 + H_2O \leftrightarrow CO + 3H_2$ $\quad - \Delta H^{O}_{298} = -206$ kj/mol **(II.11)**

and producing synthesis gas by the direct partial oxidation :

$CH_4 + ½\ O_2 \leftrightarrow CO + 2H_2$ $\quad -\Delta H^{O}_{298} = 36$ kj/mol **(II.12)**

The overall reaction by synthesis gas that [2]:

$CO + 2H_2 \leftrightarrow CH_3OH$ $-\Delta H^O_{298} = -90.8$ kj/mol **(II.13)**

$CO_2 + 3H_2 \leftrightarrow CH_3OH + H_2O$ $-\Delta H^O_{298} = -49.6$ kj/mol **(II.14)**

Since the indirect conversion of methane to methanol via synthesis gas requires high temperature and pressure, researches focus on direct methods that enable to convert methane to methanol without the expensive syngas step. For that purpose catalyst development has played a crucial role in the advances that have occurred but until that date that have not been successful. For the conversion, both homogeneous and heterogeneous catalysts are used but the number of homogeneously catalyzed processes have been steadily growing in the eighties and nineties [4]. These catalysts are used for functionalization of methane (C-H bond activation) which is significant practical interest because the methane is unreactive, as be mentioned before.

II.4.2 Methane Functionalization (CH Activation)

CH activation may be defined as a reaction that cleaves a carbon-hydrogen bond. It can be considered to be the binding of a substrate to a metal center. Often this term is restricted to reactions involving organometallic catalysts. It is generally accepted that late transition metals are more tolerant of heteroatom or halogen functionality than early transition metal catalysts. As a result, much of the focus on catalyst development has been centered on late transition metals. The catalyst which is used for selective methane functionalization are compatible with the products, generally either methanol or methyl halide, and the catalyst must be tolerant of the oxidant. Much research efforts have been devoted to design and synthesis of the catalysts that can effect CH activation [31-35]. Many of these catalysts function by the same principle [22,36]: a low oxidaiton state of the catalysts serves to activate the C-H bond of the substrate (a), the resulting metal-hydrocarbyl is oxidized generally via a net $2e^-$ processes (b), and resulting high oxidation state system is susceptible to a reducing nucleophilic addition to the hydrocarbyl ligand (c) that generates the functionalized product in Figure II.6. The challenging step is the oxidation step and hence, the C-X bond forming part of the cycle.

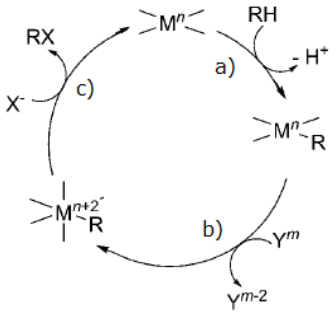

Figure II.6 General catalytic cycle for hydrocarbon functionalization using late transition metals (X=OH, Cl).

Figure II.6 depicts the three mechanisms that generally dominate discussions of C-H bond activation as oxidative addition, sigma-bond metathesis and electrophilic addition [22]. Experimental distinction between these processes is often difficult.

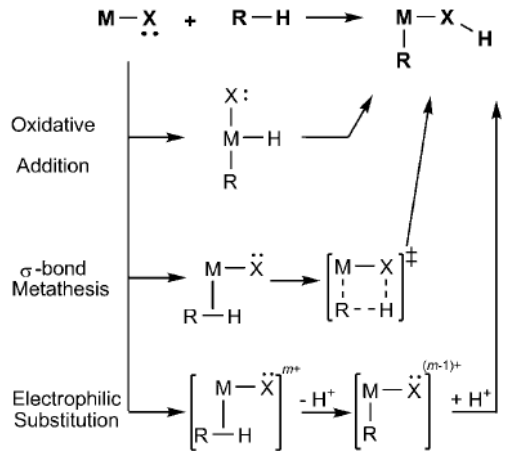

Figure II.7 "Classic" C-H bond activation mechanisms [22].

II.4.2.1 The oxidative addition

The oxidative addition of an A-B molecule such as H_2 or CH_3-I increases both the oxidaiton state and coordination number of metal centre. The oxidative addition process is often employed in catalytic cycle. The reverse reaction, reductive elimination, leads to extrusion of A-B from an M(A)(B) complex and is often the product forming step in a catalytic reaction [1,37,38].

$$\underset{16e}{L_nM} + A{-}B \underset{\text{reductive elimination}}{\overset{\text{oxidative addition}}{\rightleftharpoons}} \underset{18e}{L_nM\begin{matrix}A\\ \diagdown\\ \diagup\\ B\end{matrix}} \qquad \Delta OS = +2 \quad \Delta CN = +2 \qquad \textbf{(II.15)}$$

For transition metals the oxidative addition decreases the amount ‘n’ in the d orbital of the electronic configuration by often $2e^-$ fewer. In 1962, Vaska reported oxidative addition of H_2 to Ir(PPh3)2(CO)Cl (Eq. II.16).

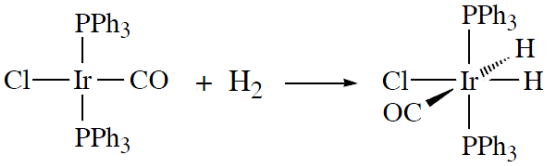

Ir (I),16e$^-$ Ir(II),18e$^-$ **(II.16)**

Table II.1: Common Types of Oxidative Addition Reaction[a]

Change in d^n Configuration	Change in Coordination Geometry	Examples	Group	Remarks
$d^{10} \rightarrow d^8$	Lin. $\xrightarrow{X_2}$ Sq. Pl.	Au(I) → (III)	11	
	Tet. $\xrightarrow{-2L, X_2}$ Sq. Pl.	Pt, Pd(0) → (II)	10	
$d^8 \rightarrow d^6$	Sq. Pl. $\xrightarrow{X_2}$ Oct.	M(II) → (IV)	10	M = Pd, Pt
		Rh, Ir(I) → (III)	9	Very common
		M(0) → (II)	8	Rare
	TBP. $\xrightarrow{-L, X_2}$ Oct.	M(I) → (III)	9	
		M(0) → (II)	8	
$d^7 \rightarrow d^6$	2Sq. Pyr. $\xrightarrow{X_2}$ 2Oct.	2Co(II) → (III)	8	Binuclear
	2Oct. $\xrightarrow{-L, X_2}$ 2Oct.	2Co(II) → (III)	8	Binuclear
$d^6 \rightarrow d^4$	Oct. $\xrightarrow{X_2}$ 7-c	Re(I) → (III)	7	
		M(0) → (II)	6	
		V(−I) → (I)	5	
$d^4 \rightarrow d^3$	2Sq. Pyr. $\xrightarrow{X_2}$ 2Oct.	2Cr(II) → (III)	6	Binuclear
	2Oct. $\xrightarrow{-L,X_2}$ 2Oct.	2Cr(II) → (III)	6	Binuclear
$d^4 \rightarrow d^2$	Oct. $\xrightarrow{X_2}$ 8-c	Mo, W(II) → (IV)	6	
$d^2 \rightarrow d^0$	Various	M(III) → (V)	5	
		M(II) → (IV)	4	

[a] Abbreviations: Lin. = linear, Tet. = tetrahedral, Oct. = octahedral, Sq. Pl. = square planar, TBP = trigonal bipyramidal, Sq. Pyr. = square pyramidal; 7-c, 8-c = 7- and 8-coordinate

II. 4.2.2 Sigma-bond metathesis

Sigma-bond metathesis is apparent oxidative addition-reductive elimination sequences. These are best recognized for d^0 early metal complexes because oxidative addition is forbidden in these cases because the oxidative addition product would

exceed the maximum permitted oxidation state (18e$^-$ rule). Hence in a reaction of such a complex with H_2, the metal therefore can not follow mechanism 'a' of Figure II.6. Instead a concerted process, both b, is believed to operate [1,38].

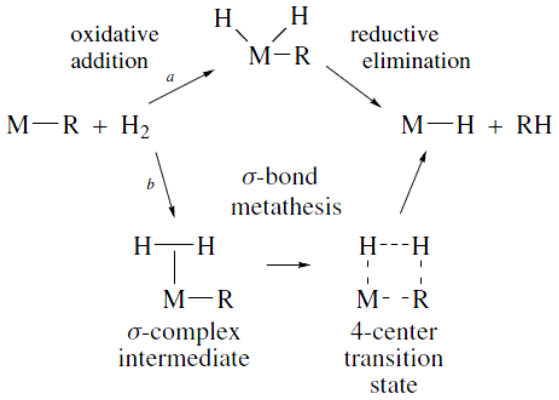

(II.17)

II.4.2.3 Electrophilic Substitution

Electrophilic substitution reactions are chemical reactions in which an electrophile, such as H^+, NO^+ displaces a group in a compound [22].

$$M\text{-}X \rightleftharpoons [M]^+[X]^- \overset{R\text{-}H}{\rightleftharpoons} [M(RH)]^+[X]^- \rightleftharpoons M\text{-}R + H\text{-}X \quad (X = Cl,...) \qquad \textbf{(II.18)}$$

II.4.3 Methane Functionalization to Methanol Using Heterogeneous Catalysts

For transformations using heterogeneous catalysts, temperatures usually exceed 250^{O}C, and the catalysts typically function with low yield and poor selectivity. A few examples for conversion by heterogeneous catalysts [22]:

- Neumann's group reported that a bipyrimidinylplatinum-polyoxometalate hybrid complex supported on silica, $[Pt(Mebpym)Cl_2][H_4PV^2Mo_{10}O_{40}]/SiO2$, catalyzes the aerobic oxidation of methane to methanol in water under mild conditions (50-60^{O}C, 1-2 bar O_2). However this reaction is not selective for methanol, producing nearly as much as formaldehyde as methanol.
- Schüt et al. developed a solid catalyst fort he direct low temperature oxidation of methane to methanol, activity similar to the Periana bipyrimidine catalyst. This catalyst displays high selectivity for methanol.

II.4.5 Methane Functionalization to Methanol Using Homogenous Catalysts

Experimental studies on the direct partial oxidation of methane to methanol over a solid catalyst have so far not been successful. Otsuka and Wang claim that the reason why CH_3OH cannot be obtained at the high temperatures needed for activation of CH_4 is that CH_3OH would immediately be decomposed or oxidized into HCHO and CO_X. Catalysts that are able to activate CH_4 at lower temperatures are therefore most important for the direct synthesis of CH_3OH [39,40]. This is a very challenging problem due to the strength of the CH bond in CH_4. Activation of methane at low temperatures has been studied using homogeneous catalysis. In 1970s, Shilov showed that methane could be converted to methanol with Pt(II) and Pt(IV) complexes [41-47]. The addition of Pt(IV) to the aqueous reaction of $PtCl_4^{2-}$ with methane lead to the production of selectively oxidized species methanol and methyl chloride. This reaction is shown in Eq. II.19.

$$CH_4 + PtCl_6^{2-} + H_2O\ (Cl^-) \xrightarrow[H_2O,\ 120^{O}C]{PtCl_4^{2-}} CH_3OH\ (CH_3Cl) + PtCl_4^{2-} + 2\ HCl \qquad \textbf{(II.19)}$$

Shilov proposed a mechanism for platinum-catalyzed alkane oxidation consisting of three basic transformation [42]:

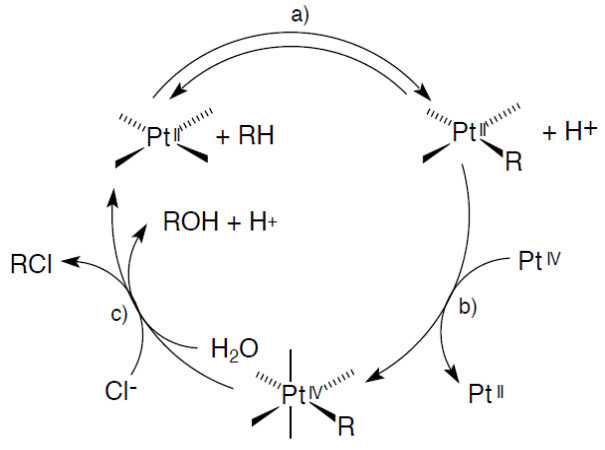

Figure II.8 Proposed mechanism for Shilov's platinum catalyzed alkane oxidation [42].
a) activation of the alkane by Pt^{II} to generate an alkyl-$platinum^{II}$ intermediate, b) two-electron oxidation of the alkyl $platinum^{II}$ intermediate to generate an alkyl-$platinum^{IV}$ species, and c) reductive elimination of RX (X= Cl or OH) to liberate the

oxidized alkane and Pt(II) catalyst. In principle, this cycle applies to the oxidation of all hydrocarbons.

Periana et al. made Shilov-like chemistry which is much more efficient in a series of methane conversion catalysts. Organometallic approaches to methane conversion became a subject mainly after the work at Periana et al. The process involves concentrated H_2SO_4 and Hg(II) complex as a catalysts [39]:

$$CH_4 + 2\ H_2SO4 \longrightarrow CH_3OSO_3 + SO_2 + 2\ H_2O \qquad \textbf{(II.20)}$$

According to Periana et al. methyl bisulfate can readily be hydrolized to methanol:

$$CH_3OSO_3H + H_2O \longrightarrow CH_3OH + H_2SO_4 \qquad \textbf{(II.21)}$$

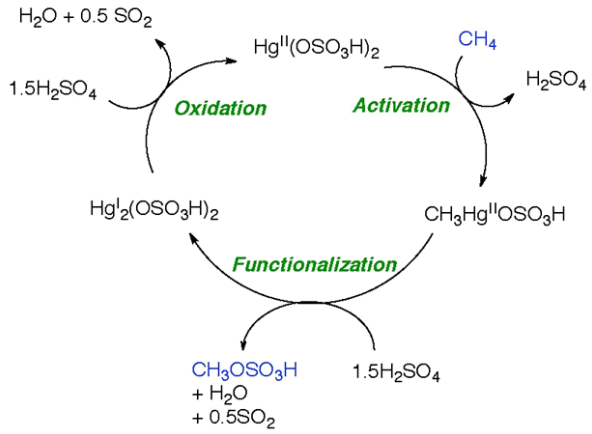

Figure II.9 Reaction mechanism for the oxidation of methane to methyl bisulfate using a Hg(II) complex in concentrated sulfuric acid [39].

In this catalytic process , overall, 50% methane conversion and 85% selectivity for the formation of methyl bisulfate were observed.

A bipyrimidyl platinum (II) complex has also been used as catalyst instead of the mercury complex in fuming sulfuric acid and the high yield of methanol obtained. The catalytica process is remarkable [Eqs. (II.22-II.25)].

$$CH_4 + H_2SO_4 + SO_3 \longrightarrow CH_3OSO_3H + H_2O + SO_2 \qquad \textbf{(II.22)}$$

$$CH_3OSO_3H + H_2O \longrightarrow CH_3OH + H_2SO_4 \qquad \textbf{(II.23)}$$

$$SO_2 + ½\ O2 \longrightarrow SO_3 \qquad \textbf{(II.24)}$$

$$\text{net reaction: } CH_4 + ½\ O_2 \longrightarrow CH_3OH \qquad \textbf{(II.25)}$$

Eq. (II.22) conversion of methane to methyl bisulfate using the Pt(II)/H_2SO_4 system, Eq. (II.23) hydrolysis of methyl bisulfate to methanol, and Eq. (II.24) reoxidation of sulfur dioxide to sulfuric acid with air could potentially be accomplished relatively inexpensively on an industrial scale.

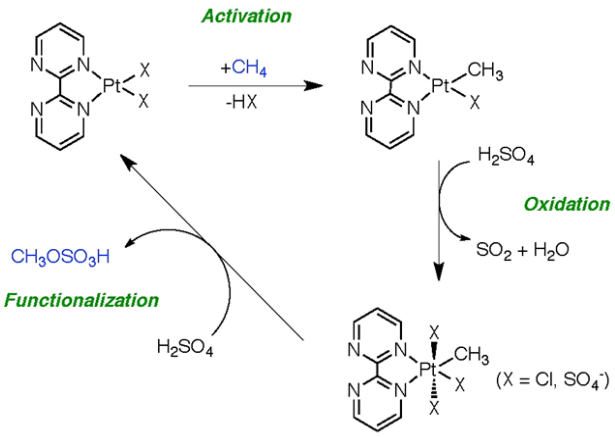

Figure II.10 Reaction mechanism for the oxidation of methane to methyl bisulfate using a bipyrimidyl Pt(II) complex in concentrated sulfuric acid [39].

In that one, the selectivity for methyl bisulfate is 81% and the conversion of methane is 89%. But in both cases, an addition step to hydrolyze methyl bisulfate to methanol is necessary.

For the activation of methane at low temperatures using homogenous catalysis has not been developed for practical applicaitons in spite of a large research effort. The direct catalytic conversion of methane remains a great challenge for the catalytic community.

CHAPTER III. MODELLING STUDIES

III.1 DENSITY FUNCTIONAL THEORY

Quantum theory is formulated in the first half of the twentieth century to describe the behavior of matter at small distance scales and radiation and the associated interactions. Several decades after the discovery of quantum mechanics further research and the availability of powerful computers make possible to apply the Quantum theory to Chemistry as well. The Nobel prize in chemistry in 1998 is shared by Professor Walter Kohn and John A. Pople. Here is a short quote from the presentation of the Nobel prize in Chemistry 1998:

"Chemistry is not only test tubes and chemicals. In quantum chemistry (computational/ theoretical chemistry), quantum mechanics is used to *compute* the properties of molecules and their interaction. This year's laureates have made it possible to use the complex equations of quantum mechanics ($\widehat{H}\Psi = E\Psi$) to study molecules and chemical processes with the help of computers. Insights that are learned about molecules via computer models provide a new and powerful methodology to understand and interpret the complexity and beauty of chemical and biochemical phenomena that we can witness each and every day." The application of quantum mechanics to chemistry is known as quantum chemistry.

The demand for sophisticated quantum chemical methods to deal with homogeneous catalysts involving transition metal complexes with their valence d shells increases as a function computing power. The oxidation and reduction of a molecule results from losing or gaining electrons respectively. Transition metal catalysts can be very useful for oxidation and reduction reactions because their outer electrons are especially susceptible to oxidation and reduction. If an oxidized transition metal runs into a molecule it can take electrons from that molecule, thereby oxidizing the molecule. If a reduced transition metal runs into a molecule it can give the molecule electrons and reduce it. Because transition metals are easier to oxidize and reduce than other elements, this process goes faster.

The computational modeling and simulations have a substantial impact on homogeneous catalysis because of recent progress in computer power and methodological algorithms. The integration of computational quantum chemistry with current research has played a significant role in the rapid development of homogeneous catalysis with organometallics. Theoretical investigations of the

structures and reaction mechanism involving molecules were entirely at quantum mechanical level on model systems in the late 1980s. Molecular simulation and *computational quantum chemistry* with its current capabilities that could be used in a wide range of applications has been developed over the last 30–35 years. The first half of these years were spent to find efficient methods to solve Schrodinger wave equation for many electron, many particle systems like molecules.

Ziegler and coworkers studied the complete hydroformylation cycle using cobalt-carbonyl species by means of DFT methods. Frenking's group has explored a number of elementary steps in $HRh(CO)_4$ catalyzed hydroformylation [48]. Morokuma and coworkers applied ab initio calculations (HF and MP2 level) to $HRh(PH_3)(CO)_2$ complexes, whereas the groups of Cundari and de Almeida carried out studies on related $HRh(PH3)_2(CO)$ model complexes at DFT and MP4 levels, respectively. As knowledge grew, many of the problems were solved by improved models and methods, and in the early 1990s several high-accuracy studies of reactions involving transition metals appeared, albeit on rather small systems. At the same time there was a dramatic improvement in the methodological treatment of large systems when new DFT methods, including gradients of the density in the functional, were developed (Becke, 1993). This finally led to the possibility of performing high-accuracy quantum chemical applications on mechanisms of redox-active metalloenzymes. This area is approximately 5 years old [10,35].

Reaction cycles are usually multistep complicated processes, and difficult to characterize experimentally. An efficient catalytic process should proceed fastly and smoothly and because of this the involved intermediates are difficult to characterize. Computational chemistry can be the only way to access a detailed knowledge of the reaction mechanism, which can be a fundamental piece of information in the optimization and design of new processes and catalysts [49].

Computational modeling is based on recognising the relationship between a structure and its molecular properties. Therefore, if a structure can be calculated and optimised from given stoichiometries and connectivities, its molecular properties can be calculated as well. The appeal of computational chemistry lies in the easier visualisation of otherwise difficult concepts such as molecular orbitals and reaction pathways, as well as in the ability to obtain information about the geometry of molecules (bond lengths and angles, dihedral angles) and some of their thermodynamic properties [50,51].

Computational modeling can also be used to aid interpretation of spectroscopic data as well as observed selectivities of reactions. Whilst computer modeling of organic compounds is firmly established, its application in organometallic and inorganic chemistry is complicated by two factors[52]. Firstly, it can be difficult to develop a good model of the close relationship between the electronic configuration and size of the metal ion and the geometry and size of ligands in determining the geometry of coordination compounds. An accurate representation of partially filled d-orbitals, to allow for the large number of possible coordination geometries and the varied chemistry of transition metal compounds, needs to be achieved. Secondly, representing and predicting the types of bonding, particularly π- bonding between ligands and transition metals, which is rare or does not occur at all in organic systems, may be difficult within many modeling programs [53].

Quantum and molecular methods have been combined in the investigation of organometallic systems. The goal of most quantum mechanical calculations is to find a molecular orbitals and the associated energy. In contrast to molecular mechanics, no information about the geometry or molecular environment of bonds, apart from the interatomic distances, is required and the emphasis is on electronic rather than nuclear behavior. The combination of the two approaches leads to very good results. In that combination, The QM method applied to the transition metal part of the system, whereas the MM method covers the remaining parts, usually containing large ligands. Otherwise, for relatively large systems neither quantum mechanics (QM) where computational time becomes forbidding, nor molecular mechanics (MM), where transition metal interactions can be difficult to predict, produce satisfactory results, if applied on their own [53].

Most of the calculations performed in computational chemistry rely on quantum mechanics. The application of quantum mechanics to chemistry is known as quantum chemistry. The main piece of information that can be obtained from a quantum chemistry study is the energy of a system. This follows directly from the Schrödinger equation [54-57].

III.1.1 Review of Density Funtional Theory

Molecules are made up of two or more atoms *as exemplified* by Figure 1 where red boll is Oxygen, Gray bolls are Carbon and white bolls are hydrogen.

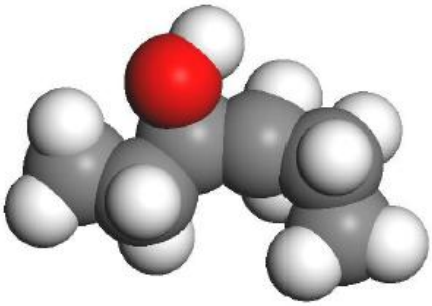

Figure III.1 An example for two or more atoms.

In quantum mechanics, a particle such as an electron, atom, or molecule, does not travel along a definite path; instead they move like a wave through space. Quantum mechanics uses wave function to describe the properties of the objects whether it is an atom, molecule or some or other form of matter. The wave is represented by the wave function, which is a central quantity in quantum theory. The wave function contains all the information that can be determined experimentally, but it is not an experimentally measurable quantity itself and is generally represented by the Greek letter psi. The wave function is complex function and depends on the coordinates of every particle in the system that it is supposed to describe. If there are N particles in the system, its wave function of in three dimensions may be represented by [49]

$$\Psi(x_1, y_1, z_1, x_2, y_2, z_2, \dots, x_{3N}, y_{3N}, z_{3N}) = \Psi(\vec{r}_1, \vec{r}_2, \dots, \vec{r}_N) \quad \textbf{(III.1)}$$

The wave functions are solutions Schrödinger's equation given by

$$\hat{H}\Psi = E \quad \textbf{(III.2)}$$

where $\hat{H}$ is the Hamiltonian of the system.

III.1.2 Born-Oppenheimer Approximation

The wave function of a molecule is a function of the coordinates of all the electrons and all the nuclei in the molecule [49].

$$\Psi(\vec{r}_1, \vec{r}_2, \dots, \vec{r}_N, \vec{R}_1, \vec{R}_2, \dots, \vec{R}_N) \quad \textbf{(III.3)}$$

where $\vec{r}_i$ and $\vec{R}_i$ represent the position vectors of the i^{th} electron and nucleus respectively. The Born-Oppenheimer approximation is based on the fact that nuclei have much larger masses than the electrons and their motions in molecules can be

separated. The Schrodinger equation can then be solved for the electrons and assume the nuclei are frozen in their instantaneous positions. This is proven to be a good approximation with many examples in the literature [54-58]. Born-Oppenheimer approximation make the wave functions depend on only of electronic coordinates, i.e $\Psi(\vec{r}_1, \vec{r}_2, \dots, \vec{r}_{N_{electrons}})$.

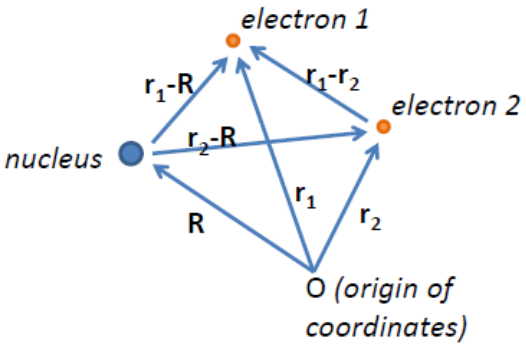

Figure III.2 Electronic coordinates of the He atom by Born-Oppenheimer approximation.

Some examples will be given in order to introduce the concept of Hamiltonian. The first example is the He atom and its Hamiltonian may be written as [49],

$$\hat{H} = \underbrace{-\frac{1}{2M}\nabla^2_{\vec{R}}}_{B.O.} \underbrace{-\frac{1}{2}\nabla^2_{\vec{r}_1}}_{\substack{kinetic\ energy\ of \\ electron\ 1}} \underbrace{-\frac{1}{2}\nabla^2_{\vec{r}_2}}_{\substack{kinetic\ energy\ of \\ electron\ 2}} \underbrace{-\frac{2}{|\vec{r}_1-\vec{R}|}}_{\substack{attraction\ of \\ electron\ 1\ by \\ He\ nucleus}} \underbrace{-\frac{2}{|\vec{r}_2-\vec{R}|}}_{\substack{attraction\ of \\ electron\ 2\ by \\ He\ nucleus}} \underbrace{+\frac{2}{|\vec{r}_1-\vec{r}_2|}}_{\substack{repulsion \\ between \\ electron\ 1 \\ and\ 2}} \quad \textbf{(III.4)}$$

The second example is for water molecule. Water contains 10 electrons and 3 nuclei. We will use the symbols "O" for the oxygen (atomic number, ZO=8) nucleus,"H_1"and"H_2"(atomic numbers ZH_1=1 and ZH_2 = 1) for the hydrogen nuclei

$$\hat{H}_{H_2O} =$$

$$\underbrace{-\frac{1}{2M_O}\nabla^2_{\vec{R}_O}}_{\substack{kinetic \\ energy\ of\ O}} \underbrace{-\frac{1}{2M_{H_1}}\nabla^2_{\vec{R}_{H_1}}}_{\substack{Kinetic \\ energy\ of\ H_1}} \underbrace{-\frac{1}{2M_{H_2}}\nabla^2_{\vec{R}_{H_2}}}_{\substack{Kinetic \\ energy\ of\ H_2}} \underbrace{-\sum_{i=1}^{10}\frac{1}{2}\nabla^2_{\vec{r}_i}}_{\substack{Kinetic\ energy \\ of\ all\ electrons}} \underbrace{-\sum_{i=1}^{10}\frac{8}{|\vec{r}_i-\vec{R}_O|}}_{\substack{electron \\ attraction \\ to\ O}} \underbrace{-\sum_{i=1}^{10}\frac{1}{|\vec{r}_i-\vec{R}_{H_1}|}}_{\substack{electron \\ attraction\ to\ H_1}}$$

$$\underbrace{-\sum_{i=1}^{10}\frac{1}{|\vec{r}_i-\vec{R}_{H_2}|}}_{\substack{electron \\ attraction\ H_2}} + \underbrace{\sum_{i=1}^{10}\sum_{j=i+1}^{10}\frac{1}{|\vec{r}_i-\vec{r}_j|}}_{\substack{electron-electron \\ repulsion}} + \underbrace{\sum_{I=1}^{3}\sum_{J=I+1}^{3}\frac{Z_I Z_J}{|\vec{R}_I-\vec{R}_J|}}_{\substack{nucleus-nucleus \\ repulsion}} \quad \textbf{(III.5)}$$

where Z_I and Z_J take the values $Z_1 = Z_O, Z_2 = Z_{H_1}$, and $Z_3 = Z_{H_2}$ [49].

As it may be seen the hamiltonial for wather molecule already complicated expression. Hamiltonians for large molecules be come even worse. Fortunately, there is a way to escape from writting such complicated and ofthen intiractable experession for Hamiltonians. Born_Oppenheimer approximation and density functional thery make it possible to have much more compact expressions that apply to any molecule, irrespectiveof its size.

In the Born-Oppenheimer approximation the nuclei are held fixed at given locations and we solve the Schrödinger equation for the wave function of the electrons alone. The resulting molecular electronic energy depends on the nuclear coordinates. Figure III.3 shows a typical electronic energy as a fuction of the distance between two nuclei. For a poly atomic molecule the electronic energy becomes a potential energy surface. A potential energy surface is a mathematical function that gives the energy of a molecule as a function of its geometry.

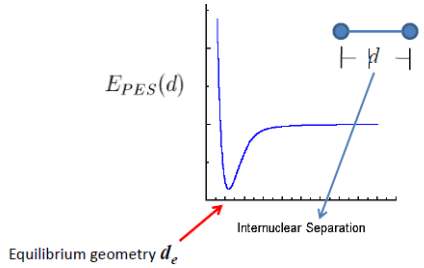

Figure III.3 A typical electronic energy as a fuction of the distance between two nuclei.

For a molecule with N_{at} and N_{el} shared by these atoms, the Born-Oppenheimer Hamiltonian may be written as in Eq. (III.6) [50]:

$$\hat{H}_{el} = \sum_{i=1}^{N}{}_{el} -\frac{1}{2}\nabla_i^2 + \sum_{i=1}^{N_{el}}\sum_{j=i+1}^{N_{el}}\frac{1}{|\vec{r}_i-\vec{r}_j|} + \sum_{i=1}^{N_{el}}\sum_{A=1}^{N_{at}}\frac{-Z_A}{|\vec{r}_i-\vec{R}_A|}$$

$$= \sum_{i=1}^{N_{el}} -\frac{1}{2}\nabla_i^2 + \sum_{i=1}^{N_{el}}\sum_{j=i+1}^{N_{el}}\frac{1}{|\vec{r}_i-\vec{r}_j|} + \sum_{i=1}^{N_{el}} V_{ext}(\vec{r}_i) \qquad \textbf{(III.6)}$$

The electrons are fermions and they posses spin angular momentum vector which is characterized by an appropriate spin quantum number. In order to uniquely describe the quantum state of an atom or molecule we also need the associated spin quantum numbers. The wave function of the system then becomes a function of both space and spin coordinates. In what follows, the space and spin coordinates will be

denoted collectively by q. In other words the following notaion fort he wave function will be used (Eq.(III.7))

$$\boldsymbol{\Psi}\left(\vec{\boldsymbol{q}}_{\boldsymbol{1}}, \vec{\boldsymbol{q}}_{\boldsymbol{2}}, \ldots, \vec{\boldsymbol{q}}_{\boldsymbol{N_{electrons}}}\right) = \boldsymbol{\Psi}\left(\boldsymbol{x_1}, \boldsymbol{y_1}, \boldsymbol{z_1}, \boldsymbol{s_1}, \boldsymbol{x_2}, \boldsymbol{y_2}, \boldsymbol{z_2}, \boldsymbol{s_2}, \ldots, \boldsymbol{x_{3N}}, \boldsymbol{y_{3N}}, \boldsymbol{z_{3N}}, \boldsymbol{s_{3N}},\right) \quad \textbf{(III.7)}$$

If the normalized wave function $\boldsymbol{\Psi}$ represents the system then its electronic electronic energy may be calculated from the integral in Eq. (III.8) [50]:

$$\boldsymbol{E_{el}} = \int \ldots \int \boldsymbol{\Psi}^* \hat{\boldsymbol{H}}_{\boldsymbol{el}} \boldsymbol{\Psi} \boldsymbol{d}\vec{\boldsymbol{q}}_{\boldsymbol{1}} \ldots \boldsymbol{d}\vec{\boldsymbol{q}}_{\boldsymbol{N_{el}}} \quad \textbf{(III.8)}$$

The Coulomb interaction between the electrons and nuclei can be looked at as an external potential for the electronic motion in density functional theory(DFT). The main reason for these assumptions comes from the fact that the BO approximation fixes the positions of nuclei and performs quantum calculation only on the electrons. Coulomb potential generated by the appositionally fixed nuclei acting on the electronic motion in a way it is an external potential in this approach as expressen in Eq. (III.9) [50].

$$\boldsymbol{E_{el}} = \int \ldots \int \boldsymbol{\Psi}^* \hat{\boldsymbol{H}}_{\boldsymbol{el}} \boldsymbol{\Psi} \boldsymbol{d}\vec{\boldsymbol{q}}_{\boldsymbol{1}} \ldots \boldsymbol{d}\vec{\boldsymbol{q}}_{\boldsymbol{N_{el}}} = \quad \textbf{(III.9)}$$

$$\int \ldots \int \boldsymbol{\Psi}^* \left(\sum_{\boldsymbol{i=1}}^{\boldsymbol{N_{el}}} -\frac{\boldsymbol{1}}{\boldsymbol{2}} \boldsymbol{\nabla}_{\boldsymbol{i}}^{\boldsymbol{2}}\right) \boldsymbol{\Psi} \boldsymbol{d}\vec{\boldsymbol{q}}_{\boldsymbol{1}} \ldots \boldsymbol{d}\vec{\boldsymbol{q}}_{\boldsymbol{N_{el}}} + \int \ldots \int \boldsymbol{\Psi}^* \left(\sum_{\boldsymbol{i=1}}^{\boldsymbol{N_{el}}} \sum_{\boldsymbol{j=i+1}}^{\boldsymbol{N_{el}}} \frac{\boldsymbol{1}}{|\vec{\boldsymbol{r}}_{\boldsymbol{i}} - \vec{\boldsymbol{r}}_{\boldsymbol{j}}|}\right) \boldsymbol{d}\vec{\boldsymbol{q}}_{\boldsymbol{1}} .. \boldsymbol{d}\vec{\boldsymbol{q}}_{\boldsymbol{N_{el}}}$$
$$+ \int \ldots \int \boldsymbol{\Psi}^* \left(\sum_{\boldsymbol{i=1}}^{\boldsymbol{N_{el}}} \boldsymbol{V_{ext}}(\vec{\boldsymbol{r}}_{\boldsymbol{i}})\right) \boldsymbol{\Psi} \boldsymbol{d}\vec{\boldsymbol{q}}_{\boldsymbol{1}} \ldots \boldsymbol{d}\vec{\boldsymbol{q}}_{\boldsymbol{N_{el}}}$$

The last term in Eq. (III.9), the energy expression represents the contribution of the interaction between the electrons and the nuclei to the electronic energy of the system. If the electronic density of the system is defined by Eq. (III.10) [50]:

$$\boldsymbol{n}(\vec{\boldsymbol{r}}) = \quad \textbf{(III.10)}$$

$$\boldsymbol{N_{el}} \int \ldots \int \boldsymbol{\Psi}^* \left(\vec{\boldsymbol{r}}, \boldsymbol{s_1}, \vec{\boldsymbol{r}}_{\boldsymbol{2}}, \vec{\boldsymbol{s}}_{\boldsymbol{2}}, \ldots, \vec{\boldsymbol{r}}_{\boldsymbol{N_{el}}}, \vec{\boldsymbol{s}}_{\boldsymbol{N_{el}}}\right) \boldsymbol{\Psi}\left(\vec{\boldsymbol{r}}, \boldsymbol{s_1}, \vec{\boldsymbol{r}}_{\boldsymbol{2}}, \vec{\boldsymbol{s}}_{\boldsymbol{2}}, \ldots, \vec{\boldsymbol{r}}_{\boldsymbol{N_{el}}}, \vec{\boldsymbol{s}}_{\boldsymbol{N_{el}}}\right) \boldsymbol{d}\vec{\boldsymbol{s}}_{\boldsymbol{1}} \boldsymbol{d}\vec{\boldsymbol{r}}_{\boldsymbol{2}} \boldsymbol{d}\vec{\boldsymbol{s}}_{\boldsymbol{2}} \ldots \boldsymbol{d}\vec{\boldsymbol{r}}_{\boldsymbol{N_{el}}} \boldsymbol{d}\vec{\boldsymbol{s}}_{\boldsymbol{N_{el}}}$$

then the last term in the above expression can be expressed as Eq. (III.11):

$$\int \ldots \int \boldsymbol{\Psi}^* \left(\sum_{\boldsymbol{i=1}}^{\boldsymbol{N_{el}}} \boldsymbol{V_{ext}}(\vec{\boldsymbol{r}}_{\boldsymbol{i}})\right) \boldsymbol{\Psi} \boldsymbol{d}\vec{\boldsymbol{q}}_{\boldsymbol{1}} \ldots \boldsymbol{d}\vec{\boldsymbol{q}}_{\boldsymbol{N_{el}}} \rightarrow \int \boldsymbol{V_{ext}}(\vec{\boldsymbol{r}}) \boldsymbol{n}(\vec{\boldsymbol{r}}) \boldsymbol{d}\vec{\boldsymbol{r}} \quad \textbf{(III.11)}$$

III.1.3 Hohenberg-Kohn Density Functional Theory

Hohenberg-Kohn (HK) Density Functional Theory replaces the wave function with the electron density which is the central theme of the theory. There are existence theorems which ensure that stationary many-particle systems can be fully characterized by their ground state density of electrons. These theorems are considered to be amongst the greatest developments in quantum theory since the Schrödinger equation in 1926. However, the actual computational methods for the density are not known and many approximations have been developed by many scientist. The first generation of approximate DFT took the shape of the exchange-correlation hole function or E_{ex} from the electron gas where the hole-function is known as a function of the electron density. This approximation became known as local DFT and it has been used extensively. Axel Becke, John Perdew and others have improved on the simple local electron gas model where the hole function correspond to an electron density that is assumed to be constant throughout. In their non-local theory the hole function or E_{ex} includes corrections from the fact that the electron density in atoms, molecules and solids changes with position. Different external potentials will always produce different densities and different densities always produce different external potentials this is illustrated in Figure III.4 [50].

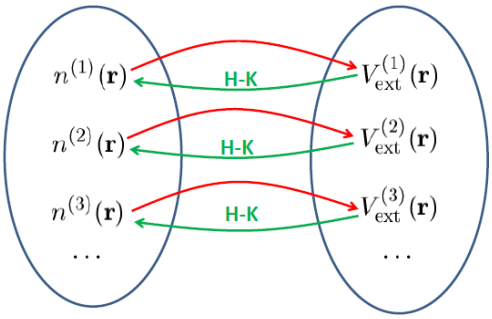

Figure III.4 Different densities always produce different external potentials.

With this understanding, it is always possible to write the electronic energy entirely as a functional of the density as seen in Eq. (III.12) [50].

(III.12)

$$E_{el=}$$

$$\int \dots \int \Psi^* \hat{H}_{el} \Psi d\vec{q}_1 \dots d\vec{q}_{N_{el}} \int \dots \int \Psi^* \left(\sum_{i=1}^{N_{el}} -\frac{1}{2}\nabla_i^2 \right) \Psi d\vec{q}_1 \dots d\vec{q}_{N_{el}} +$$

$$\int \dots \int \Psi^* \left(\sum_{i=1}^{N_{el}} \sum_{j=i+1}^{N_{el}} \frac{1}{|\vec{r}_i - \vec{r}_j|} \right) d\vec{q}_1 \dots d\vec{q}_{N_{el}} +$$

$$\int \dots \int \Psi^* \left(\sum_{i=1}^{N_{el}} V_{ext}(\vec{r}_i) \right) \Psi d\vec{q}_1 \dots d\vec{q}_{N_{el}}$$

$$=$$

$$\int \dots \int \Psi^* \left(\sum_{i=1}^{N_{el}} -\frac{1}{2}\nabla_i^2 \right) \Psi d\vec{q}_1 \dots d\vec{q}_{N_{el}} \int \dots \int \Psi^* \left(\sum_{i=1}^{N_{el}} \sum_{j=i+1}^{N_{el}} \frac{1}{|\vec{r}_i - \vec{r}_j|} \right) d\vec{q}_1 \dots d\vec{q}_{N_{el}} \rightarrow$$

$$FHK[n] \dots \Psi * i{=}1 NelVextr \Psi dq1 \dots dqNel \rightarrow Vextrnrdr$$

with these correspondence the electronic energy can be written entirely as a function of the electron density [50].

$$F_{HK}[n] + \int V_{ext}(\vec{r}) n(\vec{r}) d\vec{r} = E_{el}[n] \qquad \textbf{(III.13)}$$

Therefore, by following the derivation of Hohenberg and Kohn, it is shown that a universal functional which does not depend on external potential, $F_{HK}[n]$, exists. Unfortunately, no explicit formula is known or derived so far for the correct calculation of this functional. In order to for the theory to be useful in practice, some sort of expression is needed for the functional $F_{HK}[n]$. Perhaps a very approximate prediction would be a good starting point.

The variation principal based on the the density may be applied with the constraint that [50],

$$\int n(\vec{r}) d\vec{r} = N_{el} \qquad \textbf{(III.14)}$$

to minimize $E_{el}[n]$ in the process also derive basic DFT equation. From the solution of this equation an approximation for $E_{el}[n]$ can be optained and this result can be used to get an approximation fort he density $n(\vec{r})$. The best electronic energy is then optained by searching for the density that minimises $E_{el}[n]$.

The electronic energy of a many electron system like molecules can be separated to the following contributions as seen in Eq. (III.15) [50].

$$\boldsymbol{E_{el}} = \qquad \textbf{(III.15)}$$

$$\int \boldsymbol{\Psi}^* \left(\sum_{\boldsymbol{i=1}}^{\boldsymbol{N_{el}}} -\frac{1}{2}\nabla_i^2\right)\Psi d\vec{Q} \; +$$

$$\int \Psi^* \left(\sum_{i=1}^{N_{el}} \sum_{j=i+1}^{N_{el}} \frac{1}{|\vec{r}_i - \vec{r}_j|}\right)\Psi d\vec{Q} + \int \Psi^* \left(\sum_{i=1}^{N_{el}} V_{ext}(\vec{r}_i)\right)\Psi d\vec{Q}$$

where $d\vec{Q} = \; d\vec{q}_1 \ldots d\vec{q}_{N_{el}}$.

$$E_{el} = E_{kin} + E_{coul} + E_X + E_C + E_{ext} \qquad \textbf{(III.16)}$$

where

$$E_{kin} = \int \Psi^* \left(\sum_{i=1}^{N_{el}} -\frac{1}{2}\nabla_i^2\right)\Psi d\vec{Q}\,, E_{coul} = \; \frac{1}{2}\int\int \frac{n(\vec{r})n(\vec{r}')}{|\vec{r}-\vec{r}'|} d\vec{r}d\vec{r}', E_{ext} =$$

$Vextrnrdr$ and k_{in} stands for the kinetic energy, E_{coul} stands for the Coulomb energy, X stands for the exchange energy, C stands for the correlation energy, and ext stands for the external potential energy. The breakthrough that allows us to do DFT calculations today with high accuracy is called Kohn-Sham DFT. Kohn-Sham DFT involves the use of molecular orbitals, so it does not have the simplicity of orbital-free DFT. The rest of this course will focus on Kohn-Sham DFT. Ground state wave function may be approximated by Slater determinant for N_{el} electrons [50]:

$$\Psi_{SD}(\vec{q}_1, \vec{q}_2, \ldots, \vec{q}_{N_{el}}) = \frac{1}{\sqrt{N!}}\begin{bmatrix} \chi_1(\vec{q}_1) & \chi_2(\vec{q}_1) & \cdots & \chi_N(\vec{q}_1) \\ \chi_1(\vec{q}_2) & \chi_2(\vec{q}_2) & & \chi_N(q_2) \\ \vdots & & \ddots & \vdots \\ \chi_1(\vec{q}_{N_{el}}) & \chi_2(\vec{q}_{N_{el}}) & \cdots & \chi_N(q_{N_{el}}) \end{bmatrix} \qquad \textbf{(III.17)}$$

The density, then, can be parameterized by the one electron orbital that comprises the Slater determinant. One widely used method is the Hartree-Fock approximation to choose the one electron orbital's. There are many different functionals that can be used for E_X and E_C corrections in the literature with various degrees of sophistication. Density functional theory is implemented in both ADF and Gaussian 09 packet programs. Gaussian 09 program uses Gaussian type functions for the representation of the atomic orbitals in constructing the molecular wave functions. ADF uses Slater type orbitals for the representation of the atomic orbitals in constructing the molecular wave functions. Slater basis *functions resemble* the true atomic orbitals more closely than Gaussian basis *function.*

In the application of DFT method the most important concern is the finding of a suitable basis set along with the exchange-correlation functional $F_{XC.}$ Considerable amount of manpower and resources have been used to develop functionals that improve the uniform gas description of the LDA approach. Some examples will be breifly discussed.

Using the latter (GGA) very good results for molecular geometries and ground-state energies have been achieved. Potentially more accurate than the GGA functionals are the meta-GGA functionals. These functionals include a further term in the expansion, depending on the density, the gradient of the density and the Laplacian (second derivative) of the density. Difficulties in expressing the exchange part of the energy can be relieved by including a component of the exact exchange energy calculated from Hartree–Fock theory. Functionals of this type are known as hybrid functionals. Hybrid functionals are a class of approximations to the exchange-correlation energy functional in density functional theory (DFT) that incorporate a portion of exact exchange from Hartree-Fock theory with exchange and correlation from other sources (*ab initio*, such as LDA, or empirical). A hybrid exchange-correlation functional is usually constructed as a linear combination of the Hartree-Fock exact exchange functional, E_x^{HF} [21] :

$$E_x^{HF} = \frac{1}{2}\sum_{i,j}\int\int \psi_i^*(\mathrm{r}_1)\psi_\mathrm{j}^*(\mathrm{r}_1)\frac{1}{\mathrm{r}_{12}}\psi_\mathrm{i}(\mathrm{r}_2)\psi_\mathrm{j}(\mathrm{r}_2)\mathrm{dr}_1\mathrm{dr}_2 \qquad \textbf{(III.18)}$$

and any number of exchange and correlation explicit density functionals. The parameters determining the weight of each individual functional are typically specified by fitting the functional's predictions to experimental or accurately calculated thermochemical data. The exchange functionals which are more used nowadays are probably those labeled as B (or B88) and Becke3 (or B3), the latter containing a term introducing part of the exact exchange. As for correlation functionals, one should mention those by Lee, Yang and Parr (labeled as LYP), Perdew (known as P86) and Perdew and Wang (PW91 or P91). Since the correlation and exchange functionals are in principle independent, different combinations of them can be used [14,27]. One such functional termed the Becke (3-parameter) Lee-Yang-Parr density functional (B3LYP) has been widely used during the past years. The B3LYP functional can be written as [35]:

$$F^{B3LYP} =$$

$$(1\text{-}A) * F_X^{Slater} + A * F_X^{HF} + B * F_X^{Becke} + C * F_C^{LYP} + (1\text{-}C)\, F_C^{VWN} \qquad \textbf{(III.19)}$$

where F_X^{Slater} is the Slater exchange, F_X^{HF} is the Hartree-Fock exchange, F_X^{Becke} is the gradient part of the exchange functional (Becke 1988), F_C^{LYP} is the correlation functional of Lee et al. (1988) and F_C^{VWN} is the correlation functional of Vosko et al. (1980). A, B and C are coefficients determined using a fit to experimental heats of formation (Becke, 1993), where the correlation functionals of Perdew & Wang (1992) were used instead of F_C^{VWN} and F_C^{LYP} in the expression above [35].

Table III.1 Defination of Different DFT Functionals [35].

	Local		Gradient	
Functional	Exchange	Correlation	Exchange	Correlation
BLYP	Slater	LYP	Becke	LYP
BP	Slater	VWN	Becke	Perdew86
BP86	Slater	Perdew81	Becke	Perdew86
B3LYP[a]	Slater + HF	LYP-VWN	Becke	LYP
B3P86[a]	Slater + HF	VWN	Becke	Perdew86

[a] The coefficients weighting the different terms are obtained by a fit to experimental heats of formation.

Several DFT functionals, other than B3LYP, are used in DFT applications. Some of the most frequently used functionals are described in Table III.1.

The disadvantage of DFT with respect to HF based methods has a conceptual origin. Within the Hartree-Fock framework there is a quite well defined hierarchy of methods, which define in a reliable way what one should do to improve a given result, whether if it is by including dynamic and nondynamic correlation. Within the DFT theory, one has only a list of functionals, the relative qualities of the which are mostly known from experience, and whose relative performance in front of a particular problem is sometimes difficult to predict.

III.2 COMPUTATIONAL DETAILS

When there uneven number spins in the molecular system the spin-unrestricted density functional theory (UDFT) method must be used. In this thesis both restricted and unrestricted Becke's three-parameter hybrid exchange functional and the Lee, Yang, and Parr correlation functional have been used to carry out full optimization of geometries and energy calculations for all stationary points involved in the reactions [58,59]. In all calculations, for osmium a relativistic effective core potential (RECP) is employed for replacing the chemically inert 60 core electrons ([Kr] $4d^{10}$ $4f^{14}$), and the 5s and 5p orbitals are treated explicitly along with the 5d, 6s, and 6p valence orbitals [60,61,62]. The basis set for osmium is a modified LANL2DZ double-ξ basis set plus an f-type polarization function, (341/341/41/1), where the two outermost 6p functions of the standard LANL2DZ have been replaced by a [63] split of the optimized 6p function from Couty and Hall [64-66]. The standard triple-ξ 6-311G** basis set of Pople and co-workers is used for carbon, hydrogen, and oxygen [67]. Frequency calculations are performed for all stationary points to check whether the optimized geometry corresponds to a minimum or a transition state and to obtain the zero-point vibrational energies (ZPVE) and Gibbs free energies. The total energies of all species are obtained by taking unscaled zeropoint energy corrections into account. Intrinsic reaction coordinates (IRCs) are traced from a transition state toward both reactant and product directions using the algorithm developed by Gonzalez and Schlegel in the mass-weighted internal coordinate system to verify whether the reactant and the product are really connected by the transition state [68]. All calculations have been performed using Gaussian 09 program [63,69].

Zhang et al had investigated carefully to calibrate the accuracy of the selected method in describing [Os, C, H_4]$^+$ species and their results indicated that without the inclusion of the spin/orbit effect the selected method still gives a good description on the reaction $Os^+ + CH_4$ [70]. Zhang et al calculated the ionization potential of OsO_4 is calculated to be 13.02 eV, which is very close to the experimental value 12.97 ± 0.12 eV from the mass spectrometric study [71]. Therefore, for species [OsO^+, O, C, H_n]$^+$ involved in the present work, the B3LYP method with the selected basis set should be reliable in computing the relative energies of the species involved in the title reactions.

Vibrational frequencies were also investigated using ADF sofware program in the study because of the importance of these frequencies being like a finger print to the species. All these calculations were done for the lower multiplicity. The hybrid funtion was chosen with taking B3LYP basis set.

III.3 REACTION MECHANISMS

In 1990, Schröder and Schwarz showed that gas-phase FeO^+ reacts directly and efficiently with methane and produce first the intermediary [H_2C-Fe^+-OH] then predominantly the final products $FeOH^+ + CH_3^{\bullet}$ and $Fe^+ + CH_3OH$ are formed [72]. They concluded that changes for a catalytic activation with FeO^+ are good. This observation provided the motivation for the following research on the reactions of gas-phase metal oxide cations with methane at room temperature. The first line of research was concerned mostly with the first-row transition metal oxides. It was found that metal oxide cations formed by the first four members of the first-row transition metals did not exhibit any reactivity toward methane at room temperature. The metal oxide cation formed by Mn as MnO^+ showed very efficient reactivity toward methane but the major product from this reaction is $MnOH^+ + CH_3$ and its use as catalysis in methanol production found was very inefficient, i.e., the branching ratio to methanol is less than %1[73]. Another relevant example for gas phase catalytic oxidation is the reaction of FeO^+ with methane. In terms of ethanol production, this reaction was found to be more efficient than the reaction $MnOH^+ + CH_3$ [103]. The reaction of FeO^+ with methane ocur through four possible reaction intermediates. CoO^+ and NiO^+also react with methane very efficiently [74-76]. Recent studies show that CuO^+ also interacts efficiently with methane [77].

Reactions of gas phase transition metal-oxides with methane and other alkanes for the $C-H$ bond activation provide simple model system to study the process in detail. These systems have motivated many experimental and theoretical studies as can be seen from the literature [71-77].

Irikura and Beauchamp found that the number of oxo ligands has a striking effect on the chemistry of osmium oxide cluster ions [78]. In particular, oxo ligands affect not only the reactivity but also the reaction pathways, which are presented as follows [78] :

$Os^+ + CH_4 \rightarrow Os(CH_2)^+ + H_2$ **(III.20)**

$OsO^+ + CH_4 \rightarrow OOs(CH_2)^+ + H_2$ **(III.21)**

$OsO_2^+ + CH_4 \rightarrow OOs(CH_2)^+ + H_2O$ **(III.22)**

$OsO_3^+ + CH_4 \rightarrow x$ **(III.23)**

$OsO_4^+ + CH_4 \rightarrow OsO_3(OH_2)^+ + CH_3\bullet$ **(III.24)**

In this thesis the $C-H$ bond activation and transformation of methane to other forms of chemicals is studied in the presence of OsO^+ as catalyst. In order to achieve the aim of this study, two different reaction mechanisms of gas-phase OsO^+ catalyst and CH_4 are investigated. One of the reaction channel will be as seen in Eq III.22, which is dehydrogenation channel, and the other one will be as given in Eq. III.25, which is the dehydration channel.

$OsO^+ + CH_4 \rightarrow Os(CH_2)^+ + H_2O$ **(III.25)**

III.3.1 Dehydrogenation Channel

The reaction of OsO^+ with methane can proceed with the following reaction steps shown below:

$OsO^+ + CH_4 \rightarrow OOs(CH_4)^+$ **(III.26)**

$OOs(CH_4)^+ \rightarrow [OOs \cdots H \cdots (CH_3)^+]^* \rightarrow OOsH(CH_3)^+$ **(III.27)**

$OOsH(CH_3)^+ \rightarrow [OOs \cdots H_2 \cdots (CH_2)^+]^* \rightarrow OOs(H_2)(CH_2)^+$ **(III.28)**

$OOs(H_2)(CH_2)^+ \rightarrow [H_2 \cdots OsO(CH_2)^+] \rightarrow OsO(CH_2)^+ + H_2$ **(III.29)**

First step in the channel given in step III.26 is the formation of methane complex which follows a transient state (TS) to form the methylene hydride complex as seen in step III.27. The reaction which is proposed in step III.27 is called oxidative addition; which is a process that increases both the oxidative state and coordination number of a metal center.

In step III.28 the carbon-hydrogen bond activation or C-H activation is proposed. C-H activation is known as a reaction that cleaves a C-H bond. At last in step III.29 reductive elimination of molecular hydrogen is seen.

III.3.2 Dehydration Channel

The other thermodinamically possible reaction channel is dehydration channel. The dehydration reaction channel diverges from dehydrogenation reaction after Eq. III.26. The other steps that can be in the reaction path for this channel after the formation of methane complex (III.26) is proposed with the following sequenced reactions:

$$OOs(CH_4)^+ \rightarrow^{TS} [OOs^{\cdot\cdot}H^{\cdot\cdot}(CH_3)^+] \rightarrow OOsH(CH_3)^+ \quad \textbf{(III.30)}$$

$$OOsH(CH_3)^+ \rightarrow^{TS} [H^{\cdot\cdot}OOs(CH_3)^+] \rightarrow HOOs(CH_3)^+ \quad \textbf{(III.31)}$$

In step III.31 the migration of hydride from Os to the oxo ligand to yield the hydroxyl complex $Os(OH)(CH3)^+$ is considered in this channel. Then the next C-H bond oxidatively added to the metal complex as seen in step III.32.

$$HOOs(CH_3)^+ \rightarrow^{TS} [HO^{\cdot\cdot}H^{\cdot\cdot}Os(CH_2)^+] \longrightarrow Os(H)(OH)(CH_2)^+ \quad \textbf{(III.32)}$$

$$Os(H)(OH)(CH_2)^+ \rightarrow^{TS} [H^{\cdot\cdot}HOOs(CH_2)^+] \longrightarrow Os(H_2O)(CH_2)^+ \quad \textbf{(III.33)}$$

In Eq. III.33, a reductive eliminationstep with H_2 shifting from Os to the newly formed hydroxyl ligand occurs, forming a water-coordinated complex $Os(H_2O)(CH_2)^+$. Finally, this water-coordinated complex $Os(H_2O)(CH_2)^+$ releases the water to give the final products seen in Eq. III.34.

$$Os(H_2O)(CH_2)^+ \longrightarrow Os(CH_2)^+ + H_2O \quad \textbf{(III.34)}$$

CHAPTER IV. RESULTS AND DISCUSSIONS

Theoretical studies carried out in this thesis in order to investigate the producibility of methanol from methane. Thus, simulations were carried out in this study. These simulation calculations can be classified mainly in five groups as follows:

1. Determining optimized geometries
2. Potential energy surface calculations
3. Calculation of IR Spectra
4. Calculation of thermodynamic properties
5. Kinetic studies

IV.1 DETERMINATION OF OPTIMIZED GEOMETRIES

In this study, the reaction between OsO^+ homogenous catalyst and CH_4 was investigated in detail. Two main reactions were proposed that can oxidize the C-H bond in CH_4. These reactions are discussed in detail in the previous section. For both reaction channels, geometry optimization calculations were performed for all stationary points involved in the reactions. All the optimized geometries for all the species are repeated for quartet and doublet states. The higher states had large positive gibbs energy changes. Since those reactions will be thermodynamically unfavorable, they are excluded in this study [78]. For the sake of convinience, each species is labeled with its spin multiplicity as a superscript preceding the formula. The optimized geometries were first calculated for doublet states using GAUSSIAN 09 and then repeated using ADF software program.

First the results obtained from the simulation of GAUSSIAN 09 are presented. For convinience comparison between two programs are not going to be done in this study. But both of the simulation results for the doublet state of the dehydrogenation reaction wilbe discusse further section where PES are discussed.

All the species involved in the reaction of dehydrogenation reaction are presented with their simulated minimum molecular structure in Figure IV.1 and IV.2. As it is seen in Figures IV.1 and IV.2, eventhough the molecular structure are same, their corresponding quantum states have a great role in the minimum geometry.

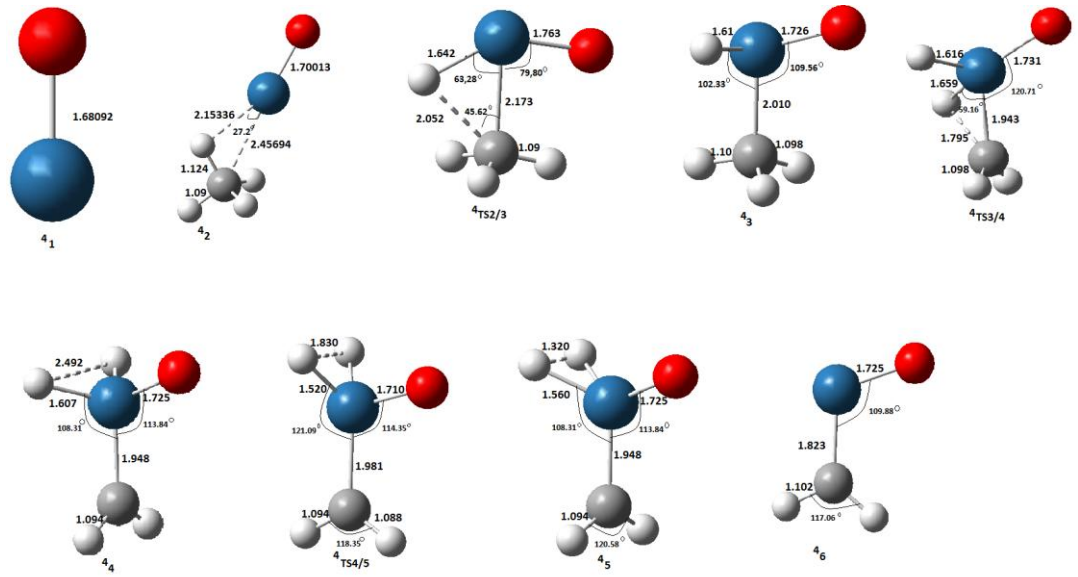

Figure IV.1 Optimized geometries for dehydrogenation reaction for the quartet quantum state.

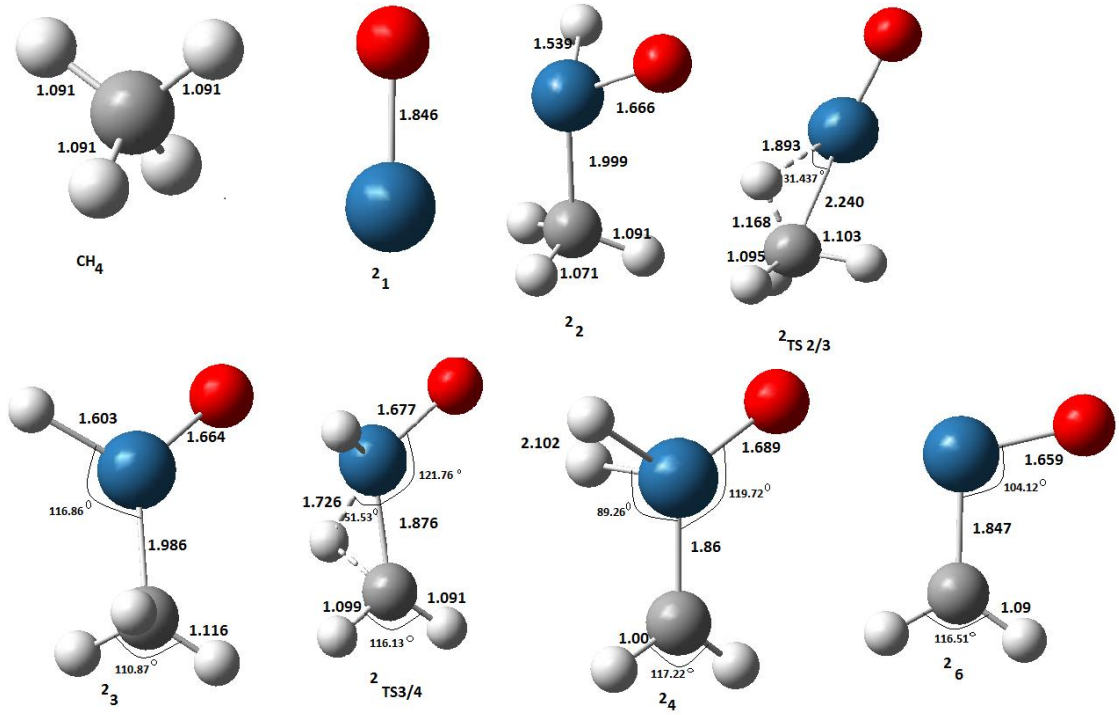

Figure IV.2 Optimized geometries for dehydrogenation reaction for the doublet quantum state.

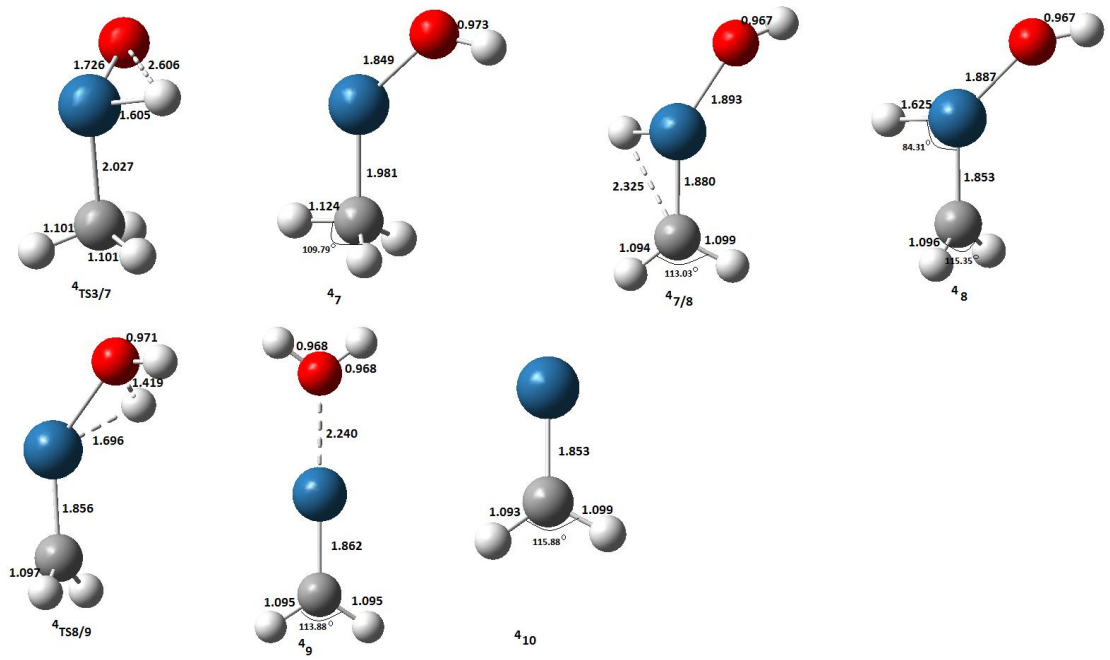

Figure IV.3 Optimized Geometries for dehydration reaction for the quantet quantum state.

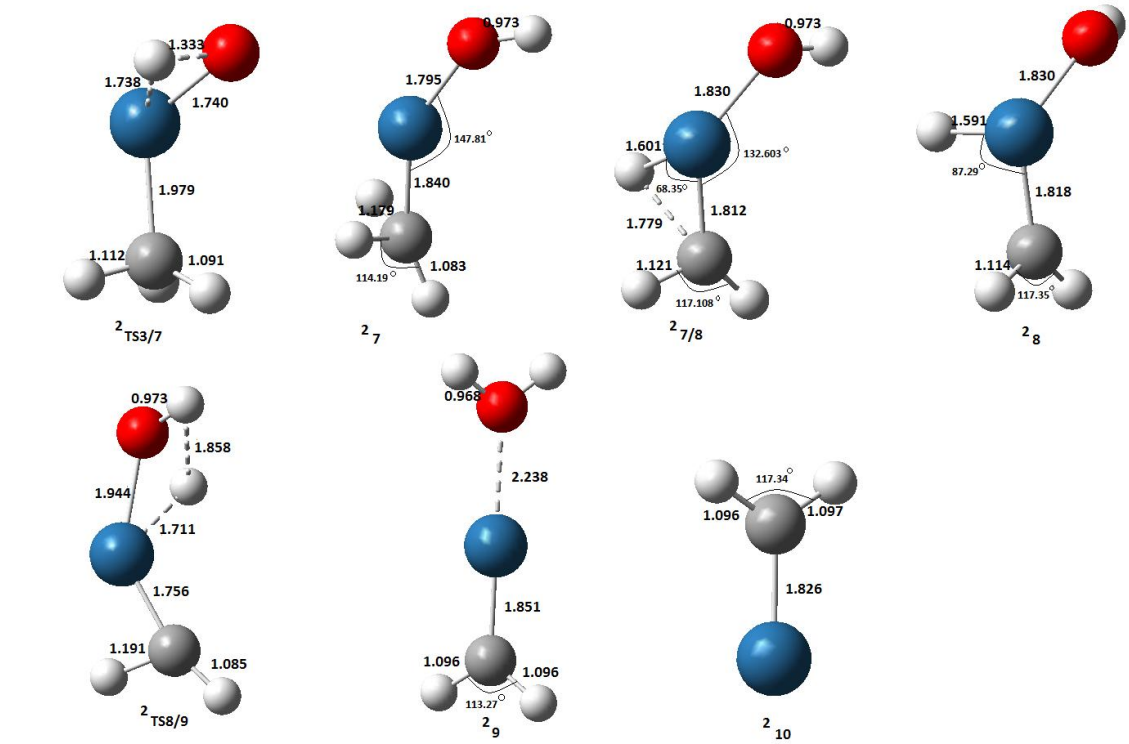

Figure IV.4 Optimized Geometries for dehydration reaction for the doublet quantum state.

All the minimum geometries given in this section will be further analyzed with their corresponding potential energy surface (PES) figures.

IV.2 POTENTIAL ENERGY SURFACE CALCULATIONS

The reaction steps in III.26-III.34 are simulated for two different spin multiplicites using the quantum chemistry software known by the name Gaussian 09. The calculational details are given in Section III.2. In the first simulation the spin multiplicity of OsO^+ cation is assumed to be quarted. In the second simulation the spin multiplicity for OsO^+ cation is assumed to be doublet. The main reason for repeating the simulation for two different multiplicities is to explore the effect of low spin ground state of OsO^+ cation versus high spin ground state on the recativity of OsO^+ cation with methane. In methane activation, the metal oxide cations tend to prefere to be in a state with high spin multiplicities to be more effective in their reaction with methane [79]. In order to satisfy the spin conservation OsO^+ cation must undergo spin flip in order to produce the first intermediary complex, $OOs(CH_4)^+$, at the end of the first reaction step (III.26). This reaction is exothermic and the enthalpy change is -23.001 kcal·mol^{-1}. This intermediary species then undergo an oxidative addition of one of its C-H bond to OsO^+cation to form the second intermediary species, $OOsH(CH_3)^+$cation, through reaction step (III.27). In this reaction step, first an extremely shallow transition state indicated by $[OOs\cdots H\cdots(CH_3)^+]^*$ is formed then the final oxidative addition reaction takes place. The reaction leading to the $OOsH(CH_3)^+$ cation doublet in step (III.27) is endothermic by 4.064 kcal·mol^{-1} relative to the end product of the reaction step (III.26). This result contradicts with the calculation presented in reference [53]. Zhang et al. predicts that the reaction step given in Eq (III.27) should be exothermic by -24.0 kcal·mol^{-1}. Reaction in step (III.28) produces Osmium methylene dihydride complex, $OOs(H_2)(CH_2)^+$ by the activation of the second C-H bond and by its subsequent oxidative addition on OsO^+. In the formation of Osmium methylene dihydride complex the reaction passes through another transition state indicated by $[OOs\cdots H_2\cdots(CH_2)^+]^*$ in the step (III.28). This transition state barrier is endothermic and the relative enthalpy change is 4.972 kcal·mol^{-1}. However the overall reaction in step (III.28) is exothermic by -5.960 kcal·mol^{-1}.

Reductive elimination, the reverse of oxidative addition, is most often seen in higher oxidation states because the formal oxidation state of the metal is reduced by two units in the reaction. In catalysis reactions, a reductive elimination is often the last step in a catalytic cycle, and the resulting fragment must be able to survive long

enough to react with the substrates for the organic reaction and so reenter the catalytic cycle. The last reaction in step (III.29) represents the reductive elimination of two hydrogen bonded to OsO^+ to form $OsO(CH_2)^+$ cation and release the Hydrogen gas, H_2. Although the final reductive elimination step is endothermic, when all the reaction steps in scheme 1 are taken into account the production H_2 gas from methane using OsO^+ catalyst is exothermic and the overall enthalpy change is negative, i.e. -10.859 kcal·mol^{-1}.

The potential energy surfaces for the reaction steps in III.26-III.29 are shown in Figure IV.5 only the beginning and the end products are in higher multiplicity.

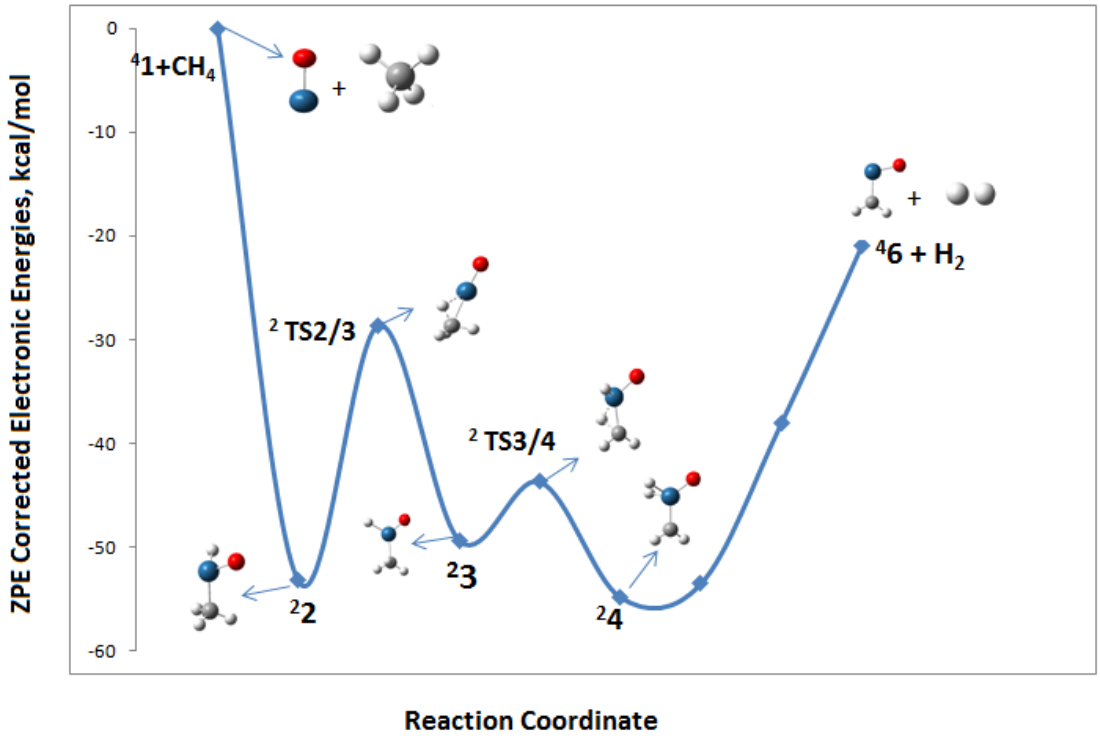

Figure IV.5 PES for the dehydrogenation reaction (spin flip over is taken into account).

Figure IV.5 represents the potential energy surface for the reaction shown in steps III.26-III.29, where OsO^+ having the multiplicities quartet at the entrance channel given in step III.26 and in the exit channel given in step III.29. When the multiplicity of the OsO^+ is changed to doublet in step III.26 and in step III.29, very similar potential surface is obtained as shown in Figure IV.6. The simulations in this study, clearly showed that the OsO^+ with doublet symmetry in the entrance and the

exit channel are more exothermic. Thus, if the spin flip would take place before the OsO^+ reacts with methane, one gets more efficient catalytic action [53].

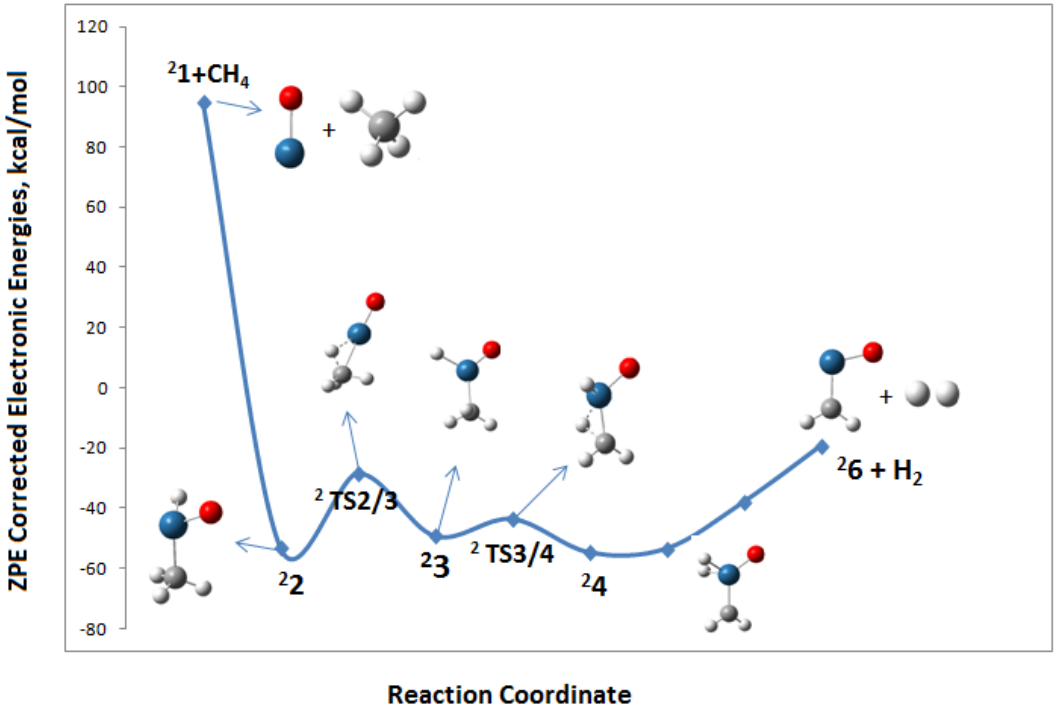

Figure IV.6 PES for the dehydrogenation reaction.

When the OsO^+ with quartet spin multiplicities starts its reaction with methane, the last step in Scheme 1 also goes through a transition state which was missing for the corresponding doublet case. This reaction is also exothermic by -10.859 kcal/mol when all steps are considered. This result is the same as the one obtained when OsO^+ starts with quartet symmetry and then reduce its multiplicity to doublet until the very last step where it recovers its quartet multiplicity again. The potential energy surface for the quartet case is shown in Figure IV.6. The transition state mentioned here is clearly visible in this figure as labeled ^{4}TS4/5.

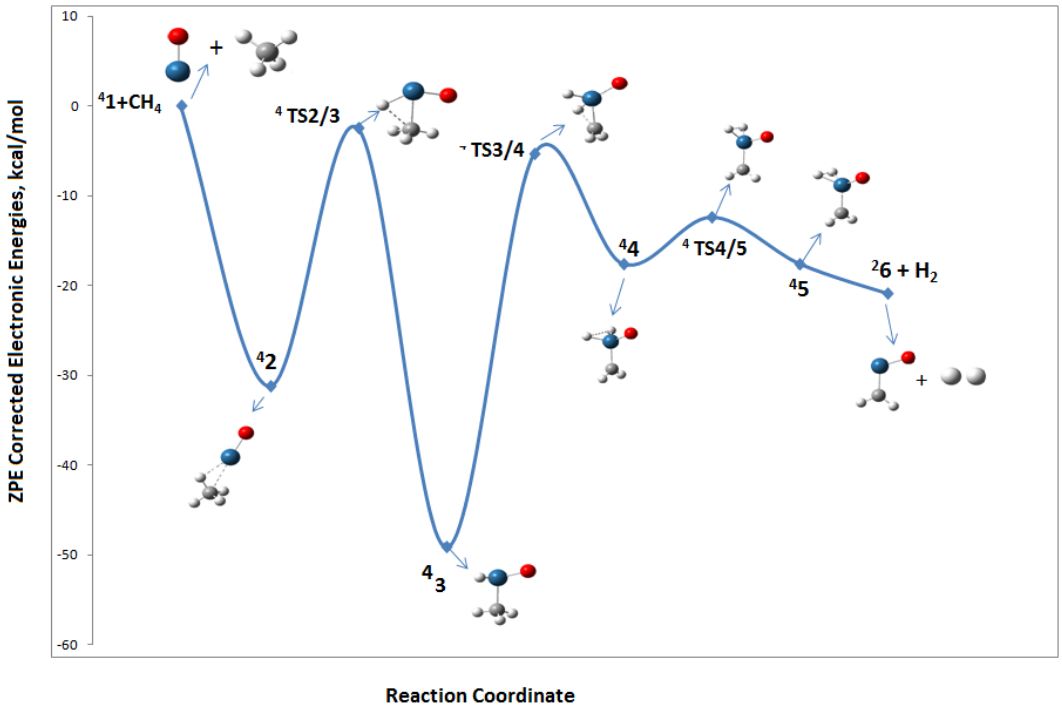

Figure IV.7. PES for the dehydrogenation reaction

IV.3 CALCULATION OF IR SPECTRA

A molecule can vibrate in many ways, and each way is called a vibrational mode. For molecules with N atoms in them, linear molecules have 3N – 5 degrees of vibrational modes, whereas nonlinear molecules have 3N – 6 degrees of vibrational modes (also called vibrational degrees of freedom). As an example H_2O, a non-linear molecule, will have $3 \times 3 - 6 = 3$ degrees of vibrational freedom, or modes.

Calculated frequencies can be used to identify intermediates (spectroscopic finger printing). It is also required for evaluating the entropy of activation in elementary reaction steps. Finally, frequency calculations can be used to generate molecular mechanics force fields for transition metal complexes.

The calculation of IR spectra were simulated in ADF program are given for the species involved in the dehydrogenation reaction because the vibrational spectroscopy does not compete with other methods of structural analysis. The advantage of these methods of spectroscopy is their extreme sensitivity to changes in molecular interaction and structure which very important to obtain the required information on the structure.

With reference to the vibrational spectrum of a compound we can typically achieve the following:

1) Detection and identification of a known compound ("fingerprinting"; tests of purity).

2) Working out the constitution of an unknown compound (presence of functional groups, e.g. Cp and CO).

3) Monitoring of chemical changes.

4) Determining the concentration of a compound (Quantitative analysis, e.g. kinetic studies involving metal carbonyls).

5) Likely structure of a molecule (use of Selection Rules and isotopic effects).

6) Normal coordinates analysis to determine the force constants of a molecule. Problems of bonding (e.g. B_2H_6).

7) Polarization measurements to determine supplementary information about molecular symmetry (e.g. in Raman) and also to study single crystals (e.g. $CaCO_3$).

The exact frequency at which a given vibration occurs is determined by the strengths of the bonds involved and the mass of the component atoms. In practice, infrared spectra do not normally display separate absorption signals for each of the 3n-6 fundamental vibrational modes of a molecule. The number of observed absorptions may be increased by additive and subtractive interactions leading to combination tones and overtones of the fundamental vibrations, in much the same way that sound vibrations from a musical instrument interact. Furthermore, the number of observed absorptions may be decreased by molecular symmetry, spectrometer limitations, and spectroscopic selection rules. One selection rule that influences the intensity of infrared absorptions is that a change in dipole moment should occur for a vibration to absorb infrared energy. Absorption bands associated with C=O bond stretching are usually very strong because a large change in the dipole takes place in that mode. The frequency scale at the bottom of the chart is given in units of reciprocal centimeters (cm^{-1}) rather than Hz, because the numbers are more manageable. Since most organic compounds have C-H bonds, a useful rule is that absorption in the 2850 to 3000 cm^{-1} is due to sp^3 C-H stretching; whereas, absorption above 3000 cm^{-1} is from sp^2 C-H stretching or sp C-H stretching if it is near 3300 cm^{-1}. The characteristics of vibrational peaks may be described by using the following general rules:

1) Stretching frequencies are higher than corresponding bending frequencies since it is easier to bend a bond than to stretch or compress it.

2) Bonds to hydrogen have higher stretching frequencies than those to heavier atoms.

3) Triple bonds have higher stretching frequencies than corresponding double bonds, which in turn have higher frequencies than single bonds.

4) Type of different vibrations may be named using the conventions given below.

a) Stretching: a change in the length of a bond, such as C-H or C-C; 

b) Bending: a change in the angle between two bonds, such as the HCH angle in a methylene group; 

c) Rocking: a change in angle between a group of atoms, such as a methylene group and the rest of the molecule.

d)Wagging: a change in angle between the plane of a group of atoms, such as a methylene group and a plane through the rest of the molecule; 

e) Twisting: a change in the angle between the planes of two groups of atoms, such as a change in the angle between the two methylene groups.

f) Out-of-plane: a change in the angle between any one of the C-H bonds and the plane defined by the remaining atoms of the ethylene molecule. Another example is in BF_3 when the boron atom moves in and out of the plane of the three fluorine atoms; 

To analyze IR spectra of all molecules in the dehydrogenation reaction, the guidelines discussed above were used. The first inverted IR peak in Figure IV.8 at 3103 cm^{-1} results from the ant-symmetric stretching motion of hydrogen on carbon where while one C-H bond is stretching away from the Carbon atom the other two are compressing toward carbon atom. The second peak at 2891cm^{-1} correspond to the symmetric stretching C-H bonds. Third peak 2273 cm^{-1} emanates from the stretching and compressing motion of the Os-H bond. Forth peak at 1390 cm^{-1} is associated with the symmetric scissoring type of vibrational motion of all the hydrogen on carbon. The overlapping peak at 1345 cm^{-1} emanates from the ant-symmetric scissoring type of vibrational motion of all the hydrogen on carbon where two hydrogens are bending forward while the other bending backward. The peak at 1025 cm^{-1} can be associated with stretching motion of Oxygen on Osmium with relatively small simultaneous rocking motion of Hydrogen on Carbon. Other peaks may also be identified with different types of vibrational motion of different groups of atoms in the molecule.

The peak located at 764 cm^{-1} is the scissoring type of vibration of the angle between C-Os-H atoms. The peak at 722 cm^{-1} is a symetric twisting motion of the CH_2 group attached to Os atom. The peak at 560 cm^{-1} is the wagging motion of the other CH_2 group. The final peak located at 150 cm^{-1} is torsional motion of the molecule around the H-Os-C-H atoms.

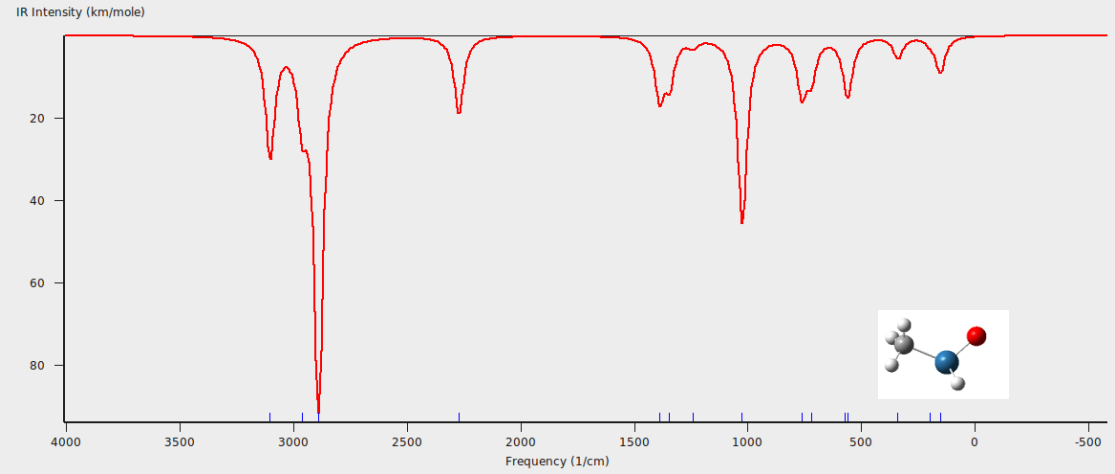

Figure IV.8 IR Spectra for the dehydrogentaion channel for doublet state for ^{2}2.

The intense imaginary pick (negative pick), can be clearly seen in Figure IV.9 for the transition state in order to produce Osmium methylene hydrid complex. In this pick the vibration of H atoms on C are vibrating very fast by coming closer and going away to Os atom.

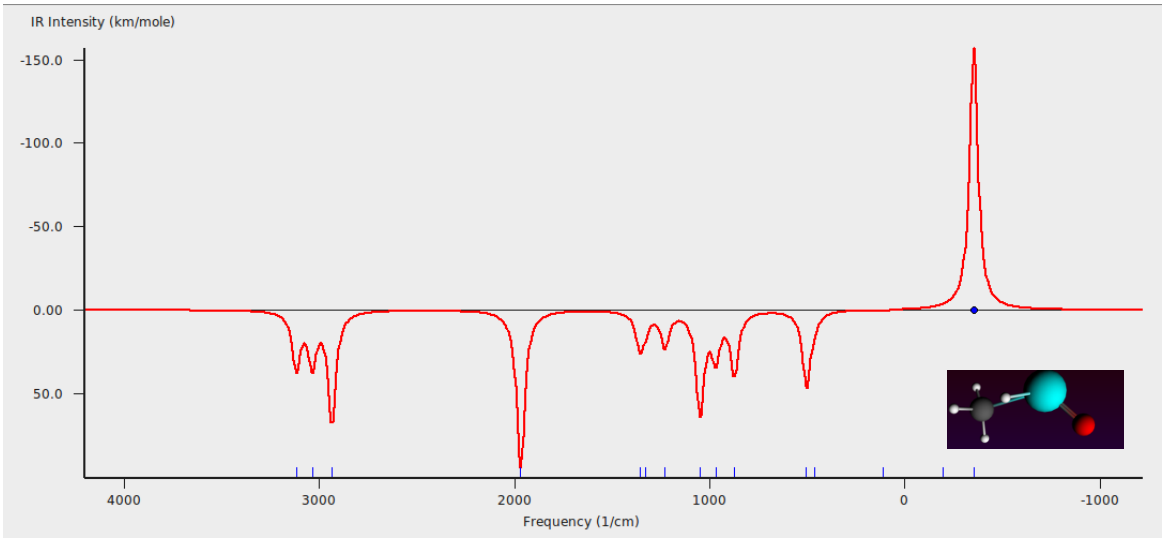

Figure IV.9 IR Spectra for the dehydrogentaion channel for doublet transition state in step Eq. III.17

In Figure IV.9, IR simulation for the produced catalyst after the transition state is shown. The first pick with frequency 3102 cm^{-1} represents the antisymmetrical stretching of hydrogens on C where one hydrogen vibrates away the other two come closer. The next and more intense pick represents the symmetrical stretching of hydrogens on C where all three hydrogens simultaneously vibrate away or come closer at 2863 cm^{-1}. Relatively weak pick at 2249 cm^{-1} represents the vibration of H on Os. The pick at 1133 cm^{-1} frequency represents the rocking motion of hydrogens on carbon around C-Os bond. The pick at 1030 cm^{-1} represents the antisimmetrical stretching of hydrogens on C and O and H on Os where while O and H on Os vibrates away hydrogens on C come closer. The pick at 542 cm^{-1} frequency represents the scissoring motion of all hydrogens on C and O and H on Os where the C-Os bond shortens while hydrogens on C and H on Os come closer.

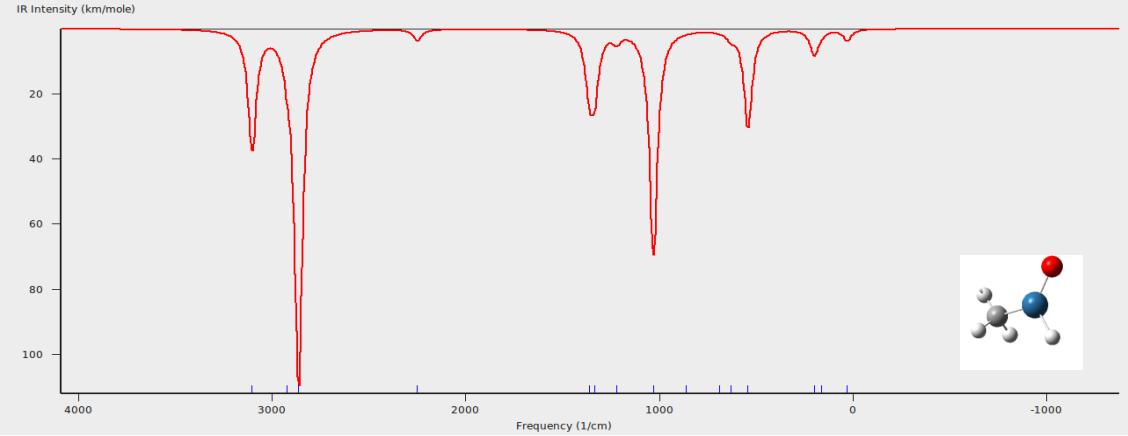

Figure IV.10 IR Spectra for the dehydrogentaion channel for doublet state for $^{2}3$

For the other species invovled in the reaction mechanism can be easily identified using these IR graphs. Since the (CH_2) is presented in all the catalyst species the pick of the vibration of two hydrogen atoms are seen around 3000 cm^{-1} frequencies as shown in Figures IV.10-11. In Figure IV.12, the IR simulation of the reactant CH_4 is given. The two characteristic vibration of all the hydrogen atoms on C is clearly seen in this figure.

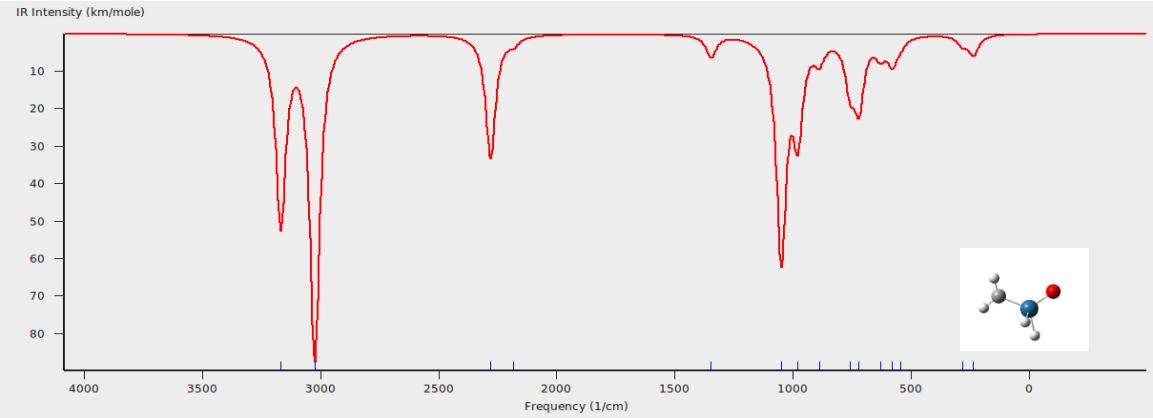

Figure IV.11 IR Spectra for the dehydrogentaion channel for doublet state for $^{2}4$

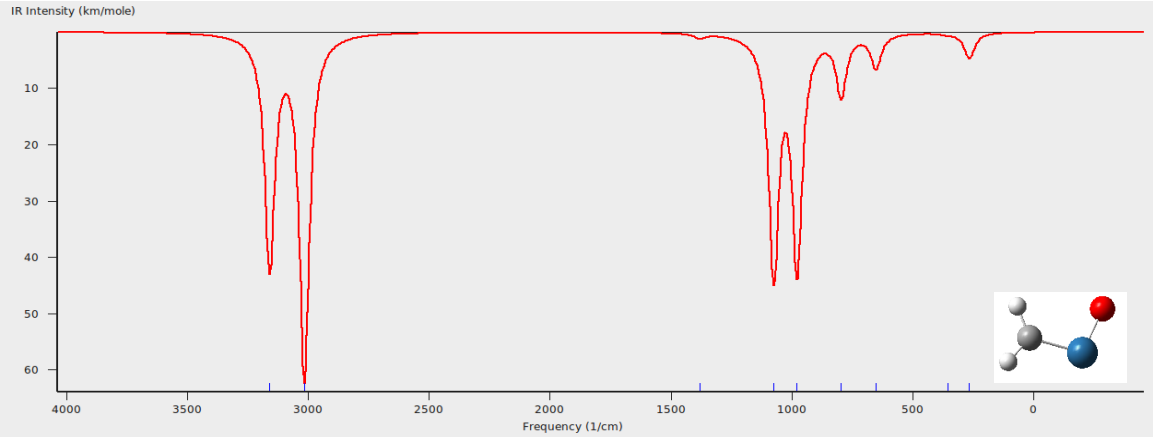

Figure IV.12 IR Spectra for the dehydrogentaion channel for doublet state for $^{2}6$.

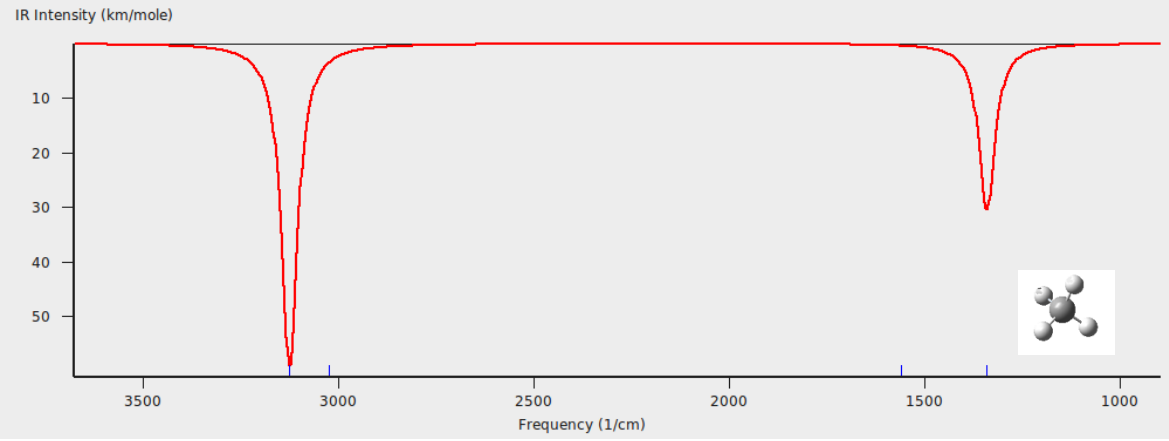

Figure IV.13 IR Spectra for the dehydrogentaion channel for doublet state for CH_4.

IV.4 CALCULATION OF THERMODYNAMIC PROPERTIES

Simulations were perfomed for the thermodynamic properties and changes in thermodynamic properties of the species involved in the first and last reaction steps of dehydrogenation reaction represented in Scheme 1. These simulations were

performed for only dehydrogenation reaction steps, since the it can also be realized experimentaly [53]. The change in thermodynamic potentials like enthalpy and gibbs energy are independent of reaction path. They depend only on their initial and final state values for a given reaction.

Simulations were first carried out for the reaction given below:

$$OsO^{+} + CH_4 \leftrightarrow OsO(CH_2) + H_2 \quad \textbf{(IV.1)}$$

In order to calculate the formation of gibbs and formation of enthalpies for this reaction step, formation of gibbs and formation of enthalpies must be calculated for all the species involved. In these calculations a method based on atomization energies was used to obtain the formation of enthalpy and formation of gibbs energies [Khan]. This method requires both theoretical and experimental inputs for the atomization energies of the individual atoms in every species. For a molecule of the general structural formula $C_aH_bO_cOs_d$, the method can be implemented with the following expression.

$$\Delta H^{o}_{f,298.15K}(C_aH_bO_cOs_d) = \quad \textbf{(IV.2)}$$
$$\left[a\Delta H^{o}_{f,298.15K}(C) + b\Delta H^{o}_{f,298.15K}(H) + c\Delta H^{o}_{f,298.15K}(O) + d\Delta H^{o}_{f,298.15K}(Os)\right] -$$
$$[aH^{298.15}(C) + bH^{298.15}(H) + cH^{298.15}(O) + dH^{298.15}(Os) + H^{298}(C_aH_bO_cOs_d)]$$

In applying this formula the heats of formation of atomic carbon, hydrogen, oxygen, and osmium are taken from the experiments (JANAF tables). The values taken from the JANAF tables are: $\Delta H^{o}_{f,298.15K}(C)$=171.21 kcal·mol^{-1}, $\Delta H^{o}_{f,298.15K}(H)$=52.10 kcal·mol^{-1}, $\Delta H^{o}_{f,298.15K}(O)$=59.43 kcal·mol^{-1}, $\Delta H^{o}_{f,298.15K}(Os)$=189.18 kcal·mol^{-1}. The atomization energies for the atoms $H^{298.15}(C)$, $H^{298.15}(H)$, $H^{298.15}(O)$, and $H^{298.15}(Os)$ and enthalpies for all the molecular species involved in the reaction were calculated using Gaussian 09 at the same temperature. The mathematical expression used in the actual calculations of enthalpies from Gaussian 09 is given below.

$$H^{298.15} = E_e + ZPE + E_v^{298.15} + E_{tr}^{298.15} + E_r^{298.15} + \Delta PV \quad \textbf{(IV.3)}$$

Where Ee represents the electronic energy, ZPE is the zero point vibrational energy contribution, Ev, Er, and Etr are the vibrational, the rotational, and translational energies rescpectively. ΔPV is set to be RT in th actual calculation.

After the formation of enthalpy and gibbs energies were calculated for both reactants and products the following expressions used for the calculation of the change in the enthalpies and gibbs energies of the overall reaction.

$$\Delta_{rxn}H^o(298.15K) = \sum_{prod}\Delta_f H^o_{prod}(298.15K) - \sum_{react}\Delta_f H^o_{react}(298.15K) \quad \textbf{(IV.4)}$$

$$\Delta_{rxn}G^o(298.15K) = \sum_{prod}\Delta_f G^o_{prod}(298.15K) - \sum_{react}\Delta_f G^o_{react}(298.15K) \quad \textbf{(IV.5)}$$

The atomization energies for the individual atoms are listed in Table IV.1
The calculated formation enthalpies and gibbs energies with different quantum chemistry methods are listed in Table IV.2 and 3.

Table IV.1 The calculated atomization energies

	B3PW91/6-311G(d,p)	
	Enthalpy (kcal/mol)	Gibbs (kcal/mol)
O	-17.9292	-17.9331
Os	-21.4309	-21.436
H	-313.927	-322.101
C	-23762.6	-23773.2

Table IV.2 The calculated formation of enthalpy and gibbs energies for the reactants and products for the quartet quantum state

B3PW91/6-311G(d,p)		
Species	Enthalpy (kcal/mol)	Gibbs (kcal/mol)
OsO	-576.307	-585.5194
CH_4	-20.5361	-16.80493
H_2	0.26106	0.2729353
$OsCH_2$	-611.667	-615.5766

Table IV.3 The calculated formation of enthalpy and gibbs energies for the reactants and products for the doublet quantum state

B3PW91/6-311G(d,p)		
Species	kcal/mol Enthalpy	kcal/mol Gibbs
OsO	-477.86	-486.83
CH_4	-20.54	-16.80
H_2	0.26	0.27
$OsCH_2$	-608.12	-611.60

Using Eq. IV.4 and IV.5 is easy and straight forward when one can directly access to the experimental values of formation of energies of each species. In Table IV.4 the property changes are represented.

The reaction enthalpy change seen in Table IV.4 is very close to the enthalpy change found for the reaction mechanism of dehydrogenation, which is -10.859 kcal/mol, by the B3LYP method used to calculate the PES. Thus with only 5% approximation both methods can be used to estimate the thermodynamical property changes.

Table IV.4 The thermodynamical property changes in the dehydrogenation reaction.

	Enthalpy Change of Rxn(kcal/mol)	Gibbs Change of Rxn (kcal/mol)
Multiplicity		
doublet	-109,468	-107,69
quartet	-14,5634	-12,9793

IV.5 KINETIC STUDIES

Kinetic studies were also performed in the study for the two proposed reaction mechanism; dehydrogenation and dehydration. The reaction rate constants were calculated by using the Arrhenius equation.

IV.5.1 Dehydrogenation Reaction

Two TSs were observed for the dehydrogenation having doublet multiplicity. These transition states are found for the C-H bond activation. In Figure IV.14 the plots for these reaction steps can be seen. The figure labeled as (a) represents the rate constant for the first C-H bond activation, where the other figure labeled as (b) represents the second C-H activation.

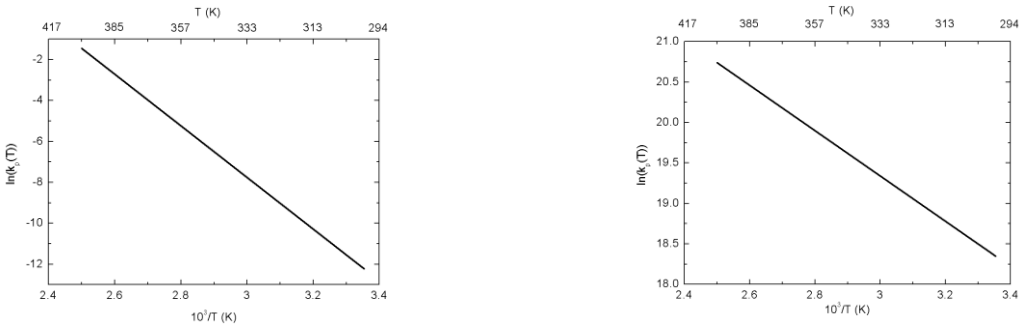

(a) (b)

Figure IV.14 The Arrhenius plot of dehydrogenation reaction for doublet state.

As can be seen from the Figure IV.14 the rate for the activation of the second C-H atom is much faster.

In Figure IV.15 the plots for dehydrogenation reaction which has quartet multiplicity can be seen. Three TSs were observed for that reaction. The figure labeled as (a) represents the rate constant for the first C-H bond activation, (b) represents the second C-H activation and (c) represents the reductively elimination.

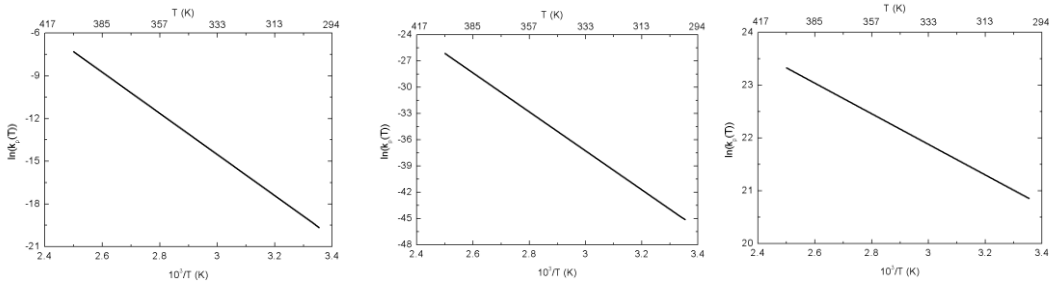

Figure IV.15 The Arrhenius plot of dehydrogenation reaction for quartet state.

From Figure IV.15, it can be say that the reductively elimination step is much faster.

IV.5.2 Dehydration Reaction

Figure IV.16 shows the plots for dehydration reaction in doublet state. Three TSs were observed for that reaction. The figure labeled as (a) represents the rate constant for the migration of the hydride from Os, (b) for the second C-H activation and (c) for the reductively elimination steps.

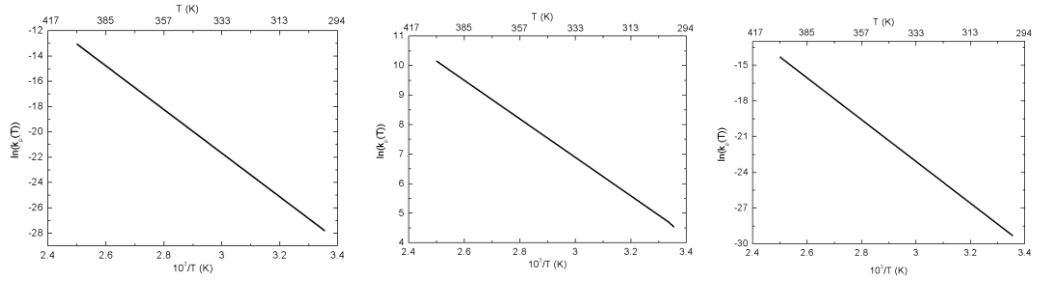

(a) (b) (c)

Figure IV.16 The Arrhenius plot of dehydration reaction mechanism for doublet state.

As can be seen from Figure IV.16, the rate for the activation of the second C-H atom is much faster.

Figure IV.17 shows the plots for dehydration reaction in quartet state. Three TSs were observed for that reaction as same as the reaction in doublet state. The

figure labeled as (a) represents the rate constant for the migration of the hydride from Os, (b) for second C-H activation and (c) for the reductively elimination steps.

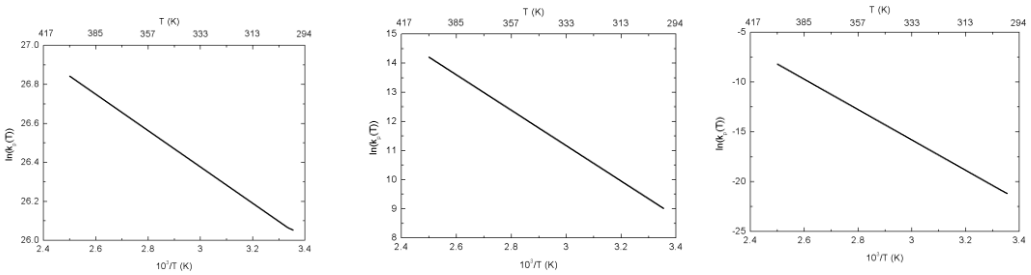

(a) (b) (c)

Figure IV.17 The Arrhenius plot of dehydration reaction mechanism for quartet state.

As can be seen from Figure IV.17, the rate of migration of hyride is much faster.

IV.6 PRELIMENARY STUDY FOR THE REACTON MECHANISM OF METHANE TO METHANOL CONVERSION

In this study, a prelimenary study for the conversion of methane to methanol has also been investigated. In Figure IV.18, the proposed reaction mechnanism can be seen.

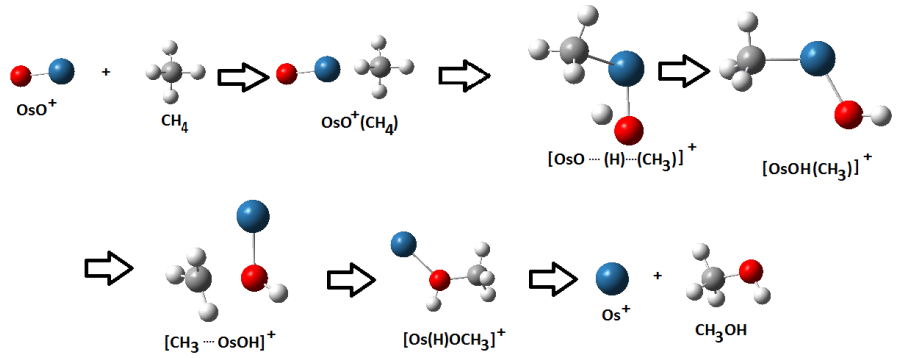

Figure IV.18 Reaction mechanism of methane to methanol conversion.

Since the lowest energy of Os atom is at quartet quantum state, the OsO^+ catalyst in the entrance channel has taken to be quartet state. Then, the spin crossover had been considered as doublet quantum state until the exit channel, and at the exit channel again the Os^+ catalyst again realized to have the second spin crossover and taken to be quartet state. Considering these quantum states, the geometry

optimizations of all the species were done in Gaussian 09 with B3LYP/6-311(d,p) method.

In Figure IV.19 the PES of the corresponding proposed reaction mechanism is given. As it can be seen from this figure, the reaction is endothermic by 25.5 kcal/mol. One of the greatest reasons for this, the optimized geometries were not scanned as the other reactions presented in this study. Thus, much more afford has to be given to this very important reaction in order to find the true geometry having the lowest energy.

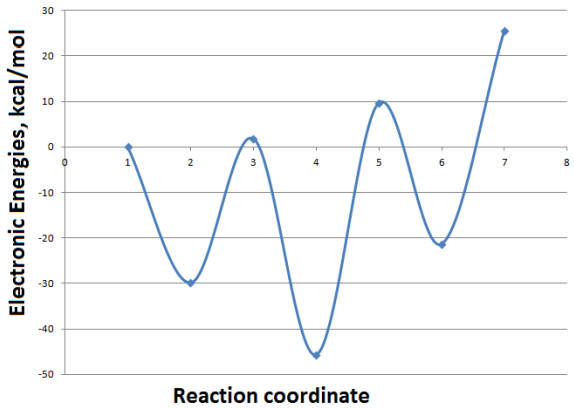

Figure IV.19 PES of the reaction mechanism of the methane to methanol conversion.

CHAPTER V. CONCLUSIONS AND RECOMMENDATIONS

V.1 CONCLUSIONS

The most important goal of this thesis was to investigate potential use of catalyst in order to activate methane. The results presented in the thesis can be summarized as follows.

1. The proposed reaction paths found to be thermodynamically reasonable.
2. The methane dehydrogenation by OsO^+ is downhill in energy on both quartet and doublet surfaces. The whole reaction on doublet path is exothermic by 113 kcal/mol, and for the quaret state it was calculated as 37 kcal/mol.
3. The overall reaction considered in spin flip is exothermic by -10.859 kcal/mol.
4. As depicted in Figures IV.5 and their corresponding optimized geometries given in Figures IV.1 and IV.2 on the quartet reaction path, the initial step is the formation of the methane complex, $OOs(CH4)^+$ given name as ^{4}**2**, which is bound by 42 kcal/mol below the entrance channel $^4OOs^+ + CH_4$.
5. The energy need for the second C-H activation found out 3 times greater for the quartet state when compared with the doublet state just needing 6.5 kcal/mol.
6. For the reaction of OsO+ with methane, the dehydrogenation channel is found to be thermodynamically and kinetically preferred.
7. In order to calculate the thermodynamical energy change using Gaussian 09, one can only perform calculations for the reactant and products only. However, to see the energy surface change of the whole reaction mechanism PESs have to be calculated for every species.
8. All the reaction steps going through transition state obeys the Arrhenius form.
9. The forward reaction rate constant is sensitive to temperature and with the increasing temperature the rate also increases. This also validated the expactations.

V.2 RECOMMENDATION

1. A preliminary study was also done in this study in order to produce CH_3OH using OsO^+ catalyst in the room temperature. However, the simple proposed reaction mechanism directly getting CH_3OH from $OsOH(CH_3)^+$ catalyst was found to be endothermic by 25.5 kcal/mol, where it is not likely to happen at room temperature. Various other mechanism steps should be searched in order to produce methanol in room temperature.
2. Other Os metal complexes having more than one O atom, like OsO_2^+, OsO_4^+, in the structure can be investigated both experimentally and theoretically.
3. Reactor modelling studies to find the most optimum conditions for various kinds of catalysists can be a very interesting chemical engineering problem and needs further attention.
4. Massive production possibilities of activation of methane to produce methanol is still a challenge. Different functionals can be choosen and compared in detail. There is still further need to understand the kinetic behavior of the C-H activation of the most stable alkane element, CH_4.

REFERENCES

[1] Crabtree, R. H.: " The Organometallic Chemistry of The Transition Metal Complexes", *John Wiley & Sons, Inc*., 4 th Edition, Canada, **(2005)** 29.

[2] Leeuwen, P.W.N.M.; Moulijin, J.A.; Santen, R.A.: "CATALYSIS : An Integrated Approach to Homogeneous, Heterogeneous and Industrial Catalysis", *Elsevier*, 79 **(1993)** 6.

[3] Sestak, J.: "Study of the kinetics of the mechanism of solid state reactions at increasing temperature.", *Thermochimica Acta*, 3 **(1971)** 1-12.

[4] Leeuwen, P.W.N.M.: "Homogeneous Catalysis : Understanding the Art", *Kluwer Academic Publishers*, the Netherlands, **(2004)** 1.

[5] Maseras, F.; Ujaque, G.: "Applications of Hybrid DFT/Molecular Mechanics to Homogeneous Catalysis", *Structure and Bonding*, 149 **(2004)** 117.

[6] Nielsen, J.R.: "Reaction Kinetics and Scale-up of Catalytic Processes", *Journal of Molecular Catalysis A : Chemical*, 163 **(2000)** 157-162.

[7] Cleland, W. W.: " The kinetics of enzym catalyzed reactions with two or more substrates or products : 1. Nomenclature and rate equations.", Biochimica et Biophsica Acta, 67 **(1963)** 104-137.

[8] Temkin, O. N.: "State-of-the-Art in the Theory of Kinetics of Complex Reactions, in Homogeneous Catalysis with Metal Complexes: Kinetic Aspects and Mechanisms", John Wiley & Sons, UK. **(2012)**.

[9] Pavlov, M.; Blomberg, M. R. A.; Siegbahn, P. E. M.; Wesendrup, R.; Heinemann, C.; Schwarz, H. *J. Phys. Chem. A*, 101 (**1997)** 1567-1579.

[10] Carr, R.W.: " Modeling of Chemical Reactions", 42 **(2007)** 1-297.

[11] **a)** Shiota, Y.; Yoshizawa, K.: "Methane to Methanol Conversion by First-Row Transition-Metal Oxide Ions: ScO^+, TiO^+, VO^+, CrO^+, MnO^+, FeO^+, CoO^+, NiO^+, and CuO^+", *J. Am. Chem. Soc.*, 122 (**2000)** 12317-12326.
b) Yoshizawa, K.; Shiota, Y.; Yamabe, T. *J.:* " Methane−Methanol Conversion by MnO^+, FeO^+, and CoO^+: A Theoretical Study of Catalytic Selectivity", *Am. Chem. Soc.*, 120 (1998) **564-572.**

[12] Robert, R.; Burwell, J.R.: "Heterogeneous Catalysis Before 1934", *American Chemical Society*, Washington, **(1983)** 3.

[13] Robertson, A.J.B.: "The Early History of Catalysis", *Platinum Metals Rev.*, 19 **(1975)** 64-69.

[14] Armor, J.N.: "A History of Industrial Catalysis", *Catalysis Today*, 163 **(2011)** 3-9.

[15] Barbaro, P.; Liguori, F.: "Heterogenized Homogeneous Catalysts for Fine Chemicals Production", *Springer,* 33 **(2010)** 1.

[16] Jagirdar, B.R.: "Transition Metal Complexes and Catalysis", *Resonance*, **(1999)** 63.

[17] Halpern, J.: "Homogeneous Catalysis by Coordination Compounds", *American Chemical Society*, Washington, **(1974)** 1.

[18] Corma, A.; Garcia, H.: "Crossing the Borders Between Homogeneous and Heterogeneous Catalysis : Developing Recoverable and Reusable Catalytic Systems", *Top Catal*, 48 **(2008)** 8-31.

[19] Herrman, W.A.; Corlins, B.: "Organometallic Homogeneous Catalysis-Quo vadis?", *Angew. Chem. Int. Ed. Engl.*, 36 **(1997)** 1048-1067.

[20] Blaser, H.U.; Indolose, A.; Schnyder, A.: "Applied Homogenous Catalysis by Organometallic Complexes", *Current Science*, 78 **(2011)** 1336.

[21] Tolman, C. A: " Steric effects of phosphorus ligands in organometallic chemistry and homogeneous catalysis", *Chemical Rewievs*, 77 **(1997)** 313-348.

[22] Bolana, T.; Gunnoe, T.B.; Webb, J.R.: "Catalytic Oxo-Functionalization of Methane and Other Hydrocarbones : Fundamental Advancements and New Strategies", *ChemSusChem* ,4 **(2011)** 37-49.

[23] Gray, D.; Tomlinson, G.; Shen, J.: "Direct Methane Conversion: An assessment", *196. American Chemical Society national meeting",* Los Angeles, **(1988)** 6.

[24] Lunsford, J.H.: " Catalytic Conversion of Methane to More Useful Chemicals and Fuels: A Challenge for 21 St Century", *Catalysis Today*, 63 **(2000)** 165-174.

[25] Crabtree, R.H.: "Organometallic alkane CH activation", *Journal of Organometallic Chemistry*, 689 **(2004)** 4083-4091.

[26] Nag, S.; Howard, J.A.K.; Sparkes, H.A.; Bhattacharya, S.: " Osmium assisted C-H activation and C=N cleavage of N-(2'-hydroxyphenyl) benzaldimines. Synthesis, structure and electrochemical properties of some organoosmium complexes", *Journal of Organometallic Chemistry*, 695 **(2010)** 2068-2075.

[27] Verma, S.S.: "To Study Direct Transformation of Methane into Methanol in the Lower Temperature Range", *Energy Conversion and Management*, 43 **(2002)** 1999-2008.

[28] Schwarz, H.: "Chemistry with Methane : Concepts Rather than Recipes", *Angew. Chem. Int. Ed.*, 50 **(2011)** 10096-10115.

[29] Torrent, M.; Sola, M.; Frenking, M.: "Theorical Studies of Some Transition-Metal-Mediated Reactions of Industrial and Synthetic Importance", *Chem. Rev.*, 100 **(2000)** 439-493.

[30] Piorier, M.G.; Sanger, A.G.; Smith, K.J.: "Direct Catalytic Conversion of Methane", *The Canadian Journal of Chemical Engineering*, 69 **(1991)** 1027-1035.

[31] Metz, R.B.: "Methane-to-Methanol Conversion by Gas-Phase Transition Metal Oxide Cations: Experiment and Theory", Department of Chemistry, University of Massachusetts, Amherst, USA.

[32] Bhalla, G.; Liu, X.Y.; Wong-Foy, A.; Jones, CJ.; Periana, R.A.: "Alkane C-H Activation by O- Donor Ir Complexes", *American Chemical Society*, **(2004)**.

[33] Periana, R.A.; Mirinov, O.; Taube, D.J.; Gamble, S.: "High Yield Conversion of Methane to Methyl Bisulfate Catalysed by Iodine Cations", *Chem. Comm.*, **(2002)** 2376-2377.

[34] Jones, CJ.; Taube, D.; Ziatdinov, V.R.; Periana, R.A.; Nielsen, R.J.; Oxgaard, J.; Goddard, W.A.: "Selective Oxidation of Methane to Methanol Catalyzed, with C-H Activation, by Homogeneous, Cationic Gold", *Angew. Chem. Int. Ed.*, 43 **(2004)** 2-5.

[35] Siegbahn, P.E.M.: "Mechanism of Metelloenzymes Studied by Quantum Mechanical Methods", *Quarterly Reviews of Biophysics*, 36 **(2003)** 91-145.

[36] Ziegler, T.; Tschinke, V.; Fan, L.; Becke, A.D.: "Theorical Study on the Electronic and Molecular Structures of $(C_5H_5)M(L)$ (M = Rh, Ir; L = CO, PH_3) and $M(CO)_4$ (M = Ru, Os) and Their Ability to Activate the C-H Bond in Methane", *J. Am. Chem. Soc.*, 111 **(1989)** 9177-9185.

[37] Collman, J.P.: "Patterns of Organometallic Reactions Related to Homogeneous Catalysis", 1 **(1968)** 136.

[38] Bhaduri, S.; Mukesh, D.: "Homogeneous Catalysis : Mechanism and Industrial Applications", *John Wiley & Sons*, **(2000)** 13.

[39] Casey, P. S.; McAllister, T.; Fogler, K.: "Selective Oxidation of Methane to Methanol at High Pressures", *Ing. Eng. Chem. Res*., 33 **(1994)** 1120-1125.

[40] Wolf, D.: "High Yields of Methanol from Methane by C-H Bond Activation at Low Temperatures", *Angew. Chem. Int. Ed.*, 37 **(1998)** 3351-3353.

[41] Holmen, A.: "Direct Conversion of Methane to Fuels and Chemicals", *Catalysis Today*, 149 **(2009)** 2-8.

[42] Goldman, A.S.; Goldberg, K.I.: "Chapter 1 : Organometallic C-H Bond Activation : An Introduction", *American Chemical Society*, **(2004)** 1.

[43] Mylvaganam, K.; Bacskay, G.B.; Hush, N.S.: "Homogeneous Conversion of Methane to Methanol. 2. Catalytic Activation of Methane by cis- and trans-Platin: A Density Functional Study of the Shilov Type Reaction", *J. Am. Chem. Soc.*, 122 **(2000)** 2041-2052.

[44] Hunt, L. B.: "The First Organometallic Compounds : William Christopher Zeise and His Platinum Complexes", *Platinum Metals Rev.*, 28 **(1984)** 76.

[45] Gerdes, G.: "Catalytic C-H Activation of Benzene by Platinum (II) : A Mechanistic Study", *Organometallics*, **(2004)**.

[46] Gerdes, G; Chen, P.: "Cationic Pt(II) Carboxlyato Complexes are Competent in Catalytic C-H Activation under Mild Conditions", *Organometallics* 23 **(2004)** 3031-3036.

[47] Gerdes, G; Chen, P.: "Comparative Gas-Phase and Solution-Phase Investigations of the Mechanism of C-H Activation by $[(N\text{-}N)Pt(CH_3)(L)]^+$", *Organometallics*, 22 **(2003)** 2217-2225.

[48] Schmid, R; Herrmann, W. A.; Frenking, G.: "Coordination Chemistry and Mechanism of Metal- Catalyzed CC-Coupling Reactions. 10. Ligand Dissociation in Rhodium – Catalyzed Hydroformylation : A theoretical Study.", Organometallics, 16 **(1997)** 701-708.

[49] James, B.; Leeuwen, P.W.N.M.: (Maseras, F.; Lledos, A.:) "Computational Modeling of Homogeneous Catalysis", *Kluwer Academic Publishers*, 25 **(2002)** 1.

[50] Cramer, C.J.: "Essentials of Computational Chemistry", *John Wiley & Sons*, 2nd Edition, **(2004)**.

[51] Van Mourik, Tanja; Gdanitz, Robert J. "A critical note on density functional theory studies on rare-gas dimers", *Journal of Chemical Physics*, 116 **(2002)** 9620–9623.

[52] G. O. Spessard and G. L. Miessler "Organometallic Chemistry", Prentice Hall, Upper Saddle River, NJ, **(1997)** 249-251.

[53] Fey, N.: "Organometallic Molecular Modelling – The Computational Chemistry of Metallocenes : A Review", *Journal of Chemical Technology and Biotechnology*, 74 **(1999)** 852-862.

[54] Schultz, N.E.; Zhao, Y.; Truhlar, D.G.: "Density Functionals for Inorganometallic and Organometallic Chemistry", *J. Phys. Chem. A.*, 109 **(2005)** 11127-11143.

[55] Eschrig, H.: "The Fundamentals of Density Functional Theory", **(2003)**.

[56] Argaman, N.; Makov, G.: "Density Functional Theory – an introduction", **(1999)** .

[57] Kohn, W.; Becke, A.D.; Parr, R.G.: "Density Functional Theory of Electronic Structure", *J. Phys. Chem.*, 100 **(1996)** 12974-12980.

[58] Becke, A. D.: "Density-functional thermochemistry. III. The role of exact exchange", *J.Chem. Phys.* **1993**, *98*, 5648-5652.

[59] Lee, C.; Yang, W.; Parr, R. G.: "Development of the Colle-Salvetti correlation energy formula into a functional of the electron density ", *Phys. Rev. B* **1988**, *37*, 785-789.

[60] Hay, P. J.; Wadt, W. R.: " *Ab initio* effective core potentials for molecular calculations. Potentials for the transition metal atoms Sc to Hg", *J. Chem. Phys.* **1985**, *82*, 270.

[61] Wadt, W. R.; Hay, P. J.: " *Ab initio* effective core potentials for molecular calculations. Potentials for main group elements Na to Bi", *J. Chem. Phys.* **1985**, *82*, 284.

[62] Hay, P. J.; Wadt, W. R.: *Ab initio* effective core potentials for molecular calculations. Potentials for K to Au including the outermost core orbitals", *J. Chem. Phys.* **1985**, *82*, 299.

[63] Gonzalez, C.; Schlegel, H. B.: " Reaction Path Following in Mass-Weighted Internal Coordinates *", J. Phys. Chem.* **1990**, *94*, 5523- 5527.

[64] LANL2DZ: Dunning D95 basis sets on first row, Los Alamos ECP plus double-*ú* basis sets on Na-Bi.

[65] Ehlers, A. W.; Böhme, M.; Dapprich, S.; Gobbi, A.; Höllwarth, A.; Jonas, A.; Köhler, K.F.; Stegmann, R.; Veldkamp, A.; Frenking, G.: "A set of f-polarization functions for pseudo-potential basis sets of the transition metals Sc – Cu, Y – Ag, and La – Au.", *Chem. Phys. Lett.* 208 **(1993)** 111-114.

[66] Couty, M.; Hall, M. B.: "Basis sets for transition metals: Optimized outer p functions", *J. Comput. Chem.* **1996**, *17*, 1359-1370.

[67] Krishnan, R.; Binkley, J. S.; Seeger, R.; Pople, J. A.: "Self-Consistent Molecular Orbital Methods. XX. A Basis Set for Correlated Wavefunctions", *J. Chem. Phys.*, 72 (**1980)** 650.

[68] Fukui, K.: " The Path of Chemical Reactions - The IRC Approach", *Acc. Chem. Res.*, 14 (**1981)** 363-368.

[69] Frisch, M. J.; Trucks, G. W.; Schlegel, H. B.; Scuseria, G. E.; Robb, M. A.; Cheeseman, J. R. Zakrzewski, V. G.; Montgomery, J. A., Jr.; Stratmann, R. E.; Burant, J. C.; Dapprich, S.; Millam, J. M.; Daniels, A. D.; Kudin, K. N.; Strain, M. C.; Farkas, O.; Tomasi, J.; Barone, V.; Cossi, M.; Cammi, R.; Mennucci, B.; Pomelli, C.; Adamo, C.; Clifford, S.; Ochterski, J.; Petersson, G. A.; Ayala, P. Y.; Cui, Q.; Morokuma, K.; Malick, D. K.; Rabuck, A. D.; Raghavachari, K.; Foresman, J. B.; Cioslowski, J.; Ortiz, J. V.; Baboul, A. G.; Stefanov, B. B.; Liu, G.; Liashenko, A.; Piskorz, P.; Komaromi, I.; Gomperts, R.; Martin, R. L.; Fox, D. J.; Keith, T.; Al-Laham, M. A.; Peng, C. Y.; Nanayakkara, A.; Challacombe, M.; Gill, P. M. W.; Johnson, B.; Chen, W.; Wong, M. W.; Andres, J. L.; Gonzalez, C.; Head-Gordon, M.; Replogle, E. S.; Pople, J. A. *GAUSSIAN 98* (release A.9); Gaussian, Inc.: Pittsburgh, PA, **(1998)**.

[70] Zhang, G. B.; Li, S. H.; Jiang, Y. S.: "Dehydrogenation of methane by gas-phase Os^+: A density functional study", *Organometallics*, *22* (**2003)** 3820-3830.

[71] Dillard, J. G.; Kiser, R. W.: "I*onization and dissociation of ruthenium and osmium tetroxides", J. Phys. Chem., 69* (**1965**) 3893- 3897.

[72] Schröder, D.; Schwarz, H.: "FeO+ Activates Methane", *Angew. Chem*., 29 **(1990)** 1433-1434.

[73] Ryan M. F.; Fiedler, A.; Schröder, D.; Schwarz, H.: "Radical-like behavior of manganese oxide cation in its gas-phase reactions with dihydrogen and alkanes.", *J. Am. Chem. Soc*., 117 **(1995)** 2033–2040.

[74] Schröder, D.; Schwarz, H.: " C-H and C-C Bond Activation by Ionic Transition-Metal Oxides in the Gas Phase", *Angew. Chem. Int. Ed. Engl.*, 34 **(1995)** 1973.

[75] Bozovic, A.; Stefan, F.; Koyanagi, G. K.; Viggiano, A. A.; Zhang, X.; Schlangen, M.; Schwarz, H.; Bohme, D. K.: " Conversion of Methane to Methanol: Nickel, Palladium, and Platinum (d9) Cations as Catalysts for the Oxidation of Methane by Ozone at Room Temperature", *Chem-Eur. J.*, 16 **(2010)** 11605.

[76] Altinay, G.; Kocak, A.; Daluz, J. S.; Metz, R. B.: "Electronic and vibrational spectroscopy of intermediates in methane-to-methanol conversion by CoO^+", *The Journal of Chemical Physics*, 135 **(2011).**

[77] Dietl, N.; C. van der Linde; Schlangen, M.; Beyer, M. K.; Schwarz, H**.:** " The Final Piece in an Intriguing Puzzle: Diatomic $[CuO]^+$ and its Role in the Spin-selective Hydrogen- and Oxygen-Atom Transfers in the Thermal Activation of Methane", Angew. Chem., Int. Ed. Engl., 50 **(2011)** 4699.

[78] Irikura, K. K.; Beauchamp, J. L.: "Osmium Tetroxide and Its Fragment Ions in the Gas Phase: Reactivity with Hydrocarbons and Small Molecules", *J. Am. Chem. Soc.* 111 **(1989)** 75-85.

[79] Metz, R. B.: " Methane-to-Methanol Conversion by Gas-Phase Transition Metal Oxide Cations: Experiment and Theory", *Research Advances in Physical Chemistry*, 2 **(2001)** 35-45.

APPENDIX A

An example for the calculation of PES

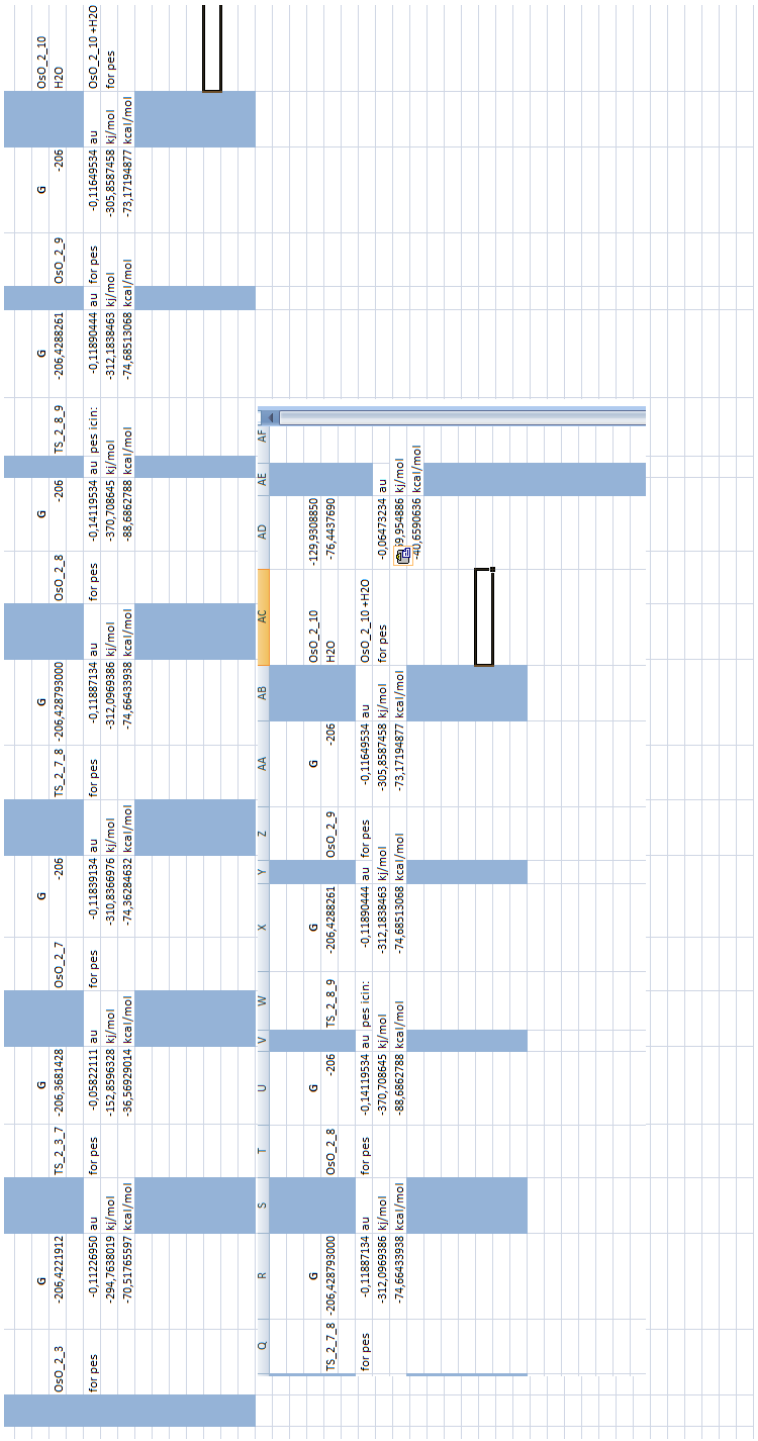

APPENDIX B

Hydrogen transfer mechanism in the ^{2}[OsOCH4] -> ^{2}[OsO(H)CH3] reaction

The calculations are performed in UB3LYP/LANL2DZ/6-311G(d,p). The optimum geometry of ^{2}[OsOCH4] within this method is as follows:

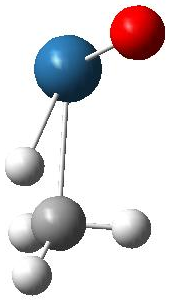

The reaction coordinate is chosen as the angle between the C-Os-H atoms. The potential energy profile for the angle is as follows:

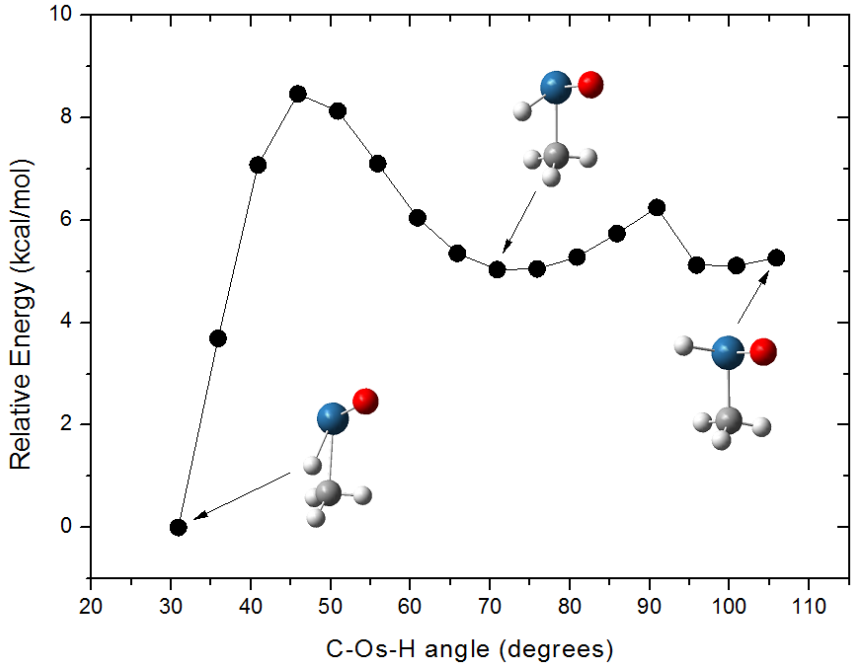

As you can see the hydrogen atom is removed from the methyl group and binds to Os atom. There is a small barrier of ~1kcal/mol from the second minimum to the third.

CURRICULUM VITAE

Figen KAYAR AYNALI has successfully gained her bachelor's degree from Cumhuriyet University in Chemical Engineering in 2010 and she then continued her Master of Science degree at the same year in Marmara University in Chemical Engineering Department. At present, she is working as a research assistant in Chemical Engineering department at the University of Yüzüncü Yıl.